OPTIMIZATION OF THE MULTI-STAGE VAPOUR COMPRESSION REFRIGERATION SYSTEM USING EIGHT LOW GWP REFRIGERANTS

A DISSERTATION
SUBMITTED IN PARTIAL FULFILMENT OF THE REQUIREMENTS
FOR THE AWARD OF THE DEGREE

OF

MASTER OF TECHNOLOGY
IN
THERMAL ENGINEERING

Submitted by:

MANJIT SINGH
2K20/THE/12

Under the supervision of

Dr AKHILESH ARORA

PROFFESOR

MECHANICAL DEPARTMENT
DELHI TECHNOLOGICAL UNIVERSITY
(Formerly Delhi College of Engineering)
Bawana Road, Delhi 110042
MAY, 2022

DELHI TECHNOLOGICAL UNIVERSITY
(Formerly Delhi College of Engineering)
Bawana Road, Delhi-110042

CANDIDATE'S DECELERATION

I, Manjit Singh, Roll No. - 2K20/THE/12, student of M. Tech Thermal Engineering, hereby declare that the project Dissertation titled "Optimization of the Multi-Stage Vapour Compression Refrigeration System Using Eight Low GWP Refrigerants" which is submitted by me to the Department of Mechanical engineering, Delhi Technological University, Delhi in partial fulfilment of the requirement for the award of the degree of Master of Technology is original and is not copied from any source proper citation. This work was not previously formed the basis for the award of any Degree, Diploma Associateship, Fellowship or other similar title or recognition.

Place: Delhi MANJIT SINGH

Date: 30/05/2022

DEPARTMENT OF MECHANICAL ENGINEERING
DELHI TECHNOLOGICAL UNIVERSITY
(Formerly Delhi College of Engineering)
Bawana Road, Delhi-110042

CERTIFICATE

I hereby certify that the Project Dissertation titled "**OPTIMIZATION OF THE MULTI-STAGE VAPOUR COMPRESSION REFRIGERATION SYSTEM USING EIGHT LOW GWP REFRIGERANTS**", which is submitted by Manjit Singh 2K20/THE/12, Mechanical Department, Delhi Technological University, Delhi in partial fulfilment of the requirement for the award of the degree of Master of Technology, is a record of the project work carried out by the student under my supervision. To the best of my knowledge, this work has not been submitted in part or full for any Degree or Diploma to this University or elsewhere.

Place: Delhi

Date: 30/05/2022

Akhilesh Arora

SUPERVISOR
Professor
Department of Mechanical Engineering
DELHI TECHNOLOGICAL UNIVERSITY
(Formerly Delhi College of Engineering)
Bawana Road, Delhi-110042

ABSTRACT

This work aims to optimize a multi-stage vapour compression refrigeration system using flash inter-cooling for different refrigerants. The performance (COP) for the system is optimized based on the evaporation temperature (T_e), condensation temperature (T_c), sub-cooling parameter (a), and de-superheating parameter (de). Eight low GWP and zero ODP refrigerants (R717, R32, R152a, R290, R41, R600a, R134a, and R1234ze(E)) are analysed for optimization at different operating conditions. Modelling of the system is accomplished using EES software. The conjugate direction method, which is generally known as the direct search method, is used to optimize the COP of the system. Research suggests that increasing the parameter "a" increases the system's COP. R717 performs better than other refrigerants with a maximum COP of 6.199, followed by R152a with a maximum COP of 6.155 for $T_{evap} = 0\ °C$, $T_{cond} = 45\ °C$, a = 1, and de = 1. When the de-superheating parameter increases, the performance of the refrigerants R717, R32, and R152a increases, R1234ze(E) and R600a show a negligible change in COP, and the rest of the refrigerants show adverse effects, i.e., COP decreases with an increase in the de-superheating parameter. The capital cost and the environmental effect are also calculated and the result shows that after optimization the total capital cost is increased and the average TEWI factor for all the eight refrigerants decreased by 40%.

Keywords: Energy; Coefficient of Performance; Sub-cooling; De-superheating; Optimization; Flash Chamber; Heat Transfer; Boiling

ACKNOWLEDGEMENT

I would like to express my deepest appreciation to all those who provided me with the possibility to go forward and complete this project. Special gratitude is due to my Head of Department, **Professor S.K. Garg** whose contribution in stimulating suggestions and encouragement, helped me to coordinate our project.

I owe a debt of gratitude to my project guide, **Dr Akhilesh Arora, Professor, Department of Mechanical Engineering, DTU**, for incorporating into me the idea of a creative Major Project, helping me in undertaking this project and also for being there whenever I needed his assistance.

I feel proud and privileged in expressing a deep sense of gratitude to all those who have helped me in presenting this project.

Last but never the least, I thank my respected parents for always being with me, in every sense.

CONTENTS

LIST OF TABLES

LIST OF FIGURES

LIST OF SYMBOLS, ABBREVIATIONS AND NOMENCLATURE

Abbreviation

COP	Coefficient of performance (−)
HFC	Hydrofluorocarbon
VCRS	Vapour-compression refrigeration system
LPC	Low-pressure compressor
ODP	Ozone depletion potential
EV	Expansion valve
GWP	Global warming potential
HPC	High-pressure compressor
NBP	Normal boiling point [°C]

Symbols

1,2,3 …	State points
evap	Evaporator
cond	Condenser
el	Electrical
in	Inlet
out	Outlet

Subscripts

T	Temperature [K]
a	Sub-cooling parameter [%]
P	Intermediate pressure [kPa]
h	Specific enthalpy [kJ/Kg]
de	De-superheating parameter [%]

W	Work input [kW]
s	Specific entropy [KJ/Kg K]
$\dot{m}$	Mass flow rate [kg/sec]
$\dot{Q}$	Heat transfer rate [kW]
h	Convective heat transfer coefficient ($W.m^{-2}. K$)

CHAPTER 1

INTRODUCTION

Heating, ventilation, and air conditioning technology have improved in many areas, including temperature manipulation for human comfort and environmental issues. In most industrial applications, vapour compression refrigeration technology is widely used. The evaporator's low-pressure vapour refrigerant is compressed and transported to the high-pressure condenser in a single step inside the compressor. In some applications, because the vapour refrigerant is already at a low temperature, the compressor's desired compression ratio is quite high, decreasing capacity. When the pressure ratio across the compressor exceeds 4 or 5, the compressor's power need rises, lowering the system performance. Multi-staging is preferable to single-stage compression for overcoming this difficulty.

1.1 LITERATURE REVIEW

Numerous theoretical and experimental research on two-stage vapour compression refrigeration systems with various configurations has been published to increase the system's overall efficiency. Nasution et al. [1] carried out a numerical investigation of VCRS under the different number of stages using R32 as a working refrigerant and compare the performance of the system with several stages their result shows that an increase in the number of stages leads to an increase in COP of the system. Gill and Singh [2] tried to find an alternate option for R134a refrigerant due to its high GWP value therefore they conduct an experimental analysis on VCRS and considered R134a/LPG and R134a as the working refrigerants, their result show that LPG/R134a performed better

in terms of COP by 15.1-17.82% under various operating conditions and conclude that R134a/LPG can be a better option in place of R134a for long-term.

Mosaffa and Farshi [3] introduced phase change materials to absorb the heat from the latent heat thermal energy storage which cools the air and the absorbed heat by the phase change material is then extracted with the help of a refrigeration system. Their results show the COP is more in the case when the cooling load is more and also concluded that the time taken by the phase change materials to solidify increases with an increase in air inlet temperature.

The refrigerating effect of a system with sub-cooling after refrigerant condensation increases, and the system's performance improves as a result. Torrella et al. [4] based on the concept of increasing refrigerating effect, presented an expression of COP for inter-stage compression systems based on sub-cooling and de-superheating and compared the results of R717 and 404A refrigerants for various configurations of an inter-stage system. Their study shows that R717 performs better than R404A and that the COP of R404A decreases as the de-superheating parameter is increased.

De Paula et al. [5] carried out the 4-E analysis of VCRS using R290, R600a, and R1234yf as working fluids and evaluate all the three costs associated with the modelling of the system and concluded that the cost rate associated with the operation of the system contributes 73% of the total cost of the system, while the penalty cost rate associated with the emission of CO_2 shows only 2.6% of contributions to the total cost and also suggested that R290 can replace R134a due to its better performance. Ahmed et al. [6] analysed single and multi-stage compression systems using lower boiling temperature refrigerants, their result showed that the model used with the sub-cooling system has a good positive impact on the energetic performance of the system and among other refrigerants used, the R22 refrigerant system performed better with maximum COP of 5.49, followed by R134a

with a COP of 5.44. Nikolaidis and Probert [7] performed an exergy-method analysis of a two-stage vapour compression refrigeration to evaluate the plant performance.

Esfahani et al. [8] performed thermodynamic and economic analysis on a multi-effect evaporation–absorption heat pump incorporated with a vapour compression system. Roy and Mandal [9] performed a full 4-E analysis of a 50kW cascade refrigeration system, a comprehensive analysis was conducted utilising four refrigerant pairs, and the results revealed that the system performed better with R41-R161 and R170-R161 refrigerant pairs in terms of minimum plant cost than with the R41-R404A pair with COP and exergetic efficiency enhancement of 4.9-7.1% and 4.5-6.6%, respectively. Arora et al. [10] presented a comprehensive thermodynamic analysis of VCRS and compared the performance of R22, R407C, and R410A. Their analysis shows that the performance of R22 is better than R407C and R410A by 3-6% at evaporator and condenser temperatures of -38°C and 40°C, respectively. Arora and Kaushik [11] considered HFC22, R410A, and R717 refrigerants and carried out optimum intermediate pressure for each refrigerant separately, and their result shows that the optimum intermediate pressure increased by 2% when there is a drop in isentropic efficiency by 10% for HFC22 and R410A, but R717 showed negligible effect on intermediate pressure with change in isentropic efficiency and concluded that R717 perform better than HFC22 and R410A in terms of exergetic efficiency.

Bhamidipati et al. [12] evaluated the usage of R32 as a possible replacement for R134a and R152a inside a refrigeration system and discovered that its coefficient of performance (COP) is approximately identical to that of R152a and is 5-7 % higher than that of R134a. Ahamed et al. [13] conducted an exergetic analysis of VCRS, their findings indicate that exergy is strongly reliant on evaporation and condensation temperatures, liquid refrigerant subcooling, dead state temperature, and compressor pressure ratio. Mancuhan [14] conducted a comprehensive comparison of refrigerants for refrigerants which are used in low-temperature applications (R717, R134A, R152A, R290, R404A, and R507A) in a two-stage compression system with the help of flash intercooling of the vapour

refrigerant and indicated that as evaporation and condensation temperatures increase, the flash chamber pressure increases in the applications where the temperature is set to be low or medium, and that for low-temperature applications, the optimum intermediate pressure is highest for the R507A system, whereas R290 system shows the low optimum intermediate pressure inside the flash chamber.

A system having sub-cooling after condensation of refrigerant results in the increase in refrigerating effect and ultimately the performance of the system increases. Torrella et al. [4] based on the concept of increasing refrigerating effect presented an expression of COP based on the sub-cooling and de-superheating for inter-stage compression systems and compared the results of R717 and 404A refrigerants for various configurations of an inter-stage system and their study shows that R717 performs better than R404A and also the COP of R404A decreased with the increase in de-superheating parameter. Singh et al. [15] used eighteen refrigerant couples in a cascade system and performed economic analysis and obtained a maximum COP of 1.917 with second law efficiency of 39.14% with R717-R290 refrigerant couple and at a minimum value of the de-superheating parameter, concluded that from an economic point of view the performance of R717-R290 is better than other refrigerant couples.

Dalkilic and Wongwises [16] performed a comparative study of vapour compression refrigeration systems using various alternate refrigerants and carried out the best performance of the system using natural refrigerants. Bilgen and Takahashi [17] performed exergy analysis and experimental study of heat pump systems. Nikolaidis and Probert [7] performed an exergy-method analysis of a two-stage vapour compression refrigeration to evaluate the plant performance. Esfahani et al. [8] performed thermodynamic and economic analysis on a multi-effect evaporation–absorption heat pump incorporated with a vapour compression system.

Roy and Mandal [9] carried out the complete 4-E analysis of a cascade refrigeration system with a cooling capacity of 50 kW, complete analysis was carried out using four refrigerants pairs, and their results showed that the system performed better with R41-R161 and R170-R161 refrigerants pairs compared to those obtained using the R41-R404A pair in terms of minimum plant cost with minimum exergy destruction rate with COP and exergetic efficiency enhancement of 4.9-7.1% and 4.5-6.6%, respectively. Arora and Kaushik [11] considered HFC22, R410A, and R717 refrigerants and carried out optimum intermediate pressure for each refrigerant separately, and their result shows that the optimum intermediate pressure increased by 2% when there is a drop in isentropic efficiency by 10% for HFC22 and R410A, but R717 showed negligible effect on intermediate pressure with change in isentropic efficiency and concluded that R717 perform better than HFC22 and R410A in terms of exergetic efficiency. Yu et al. [18] experimentally studied the boiling heat transfer inside the tube which is placed horizontally and considered two horizontal tubes of 8.4 mm and 7.9 mm diameter respectively in which five pure refrigerants were allowed to flow and with the help of correlations defined for the heat transfer, some more correlation was developed for the boiling heat transfer inside the horizontal tube. Shah [19] in his study presented two correlations of condensation for plane and mini channels in different orientations and compared the results with the result of 33 fluids which were available in the database.

According to the literature review, only a small amount of research has been published to replace R717 in low-boiling refrigerant applications. The goal of this study is to assess low-GWP refrigerants having low boiling temperatures to find a substitute for the R717 refrigerant. A multi-stage vapour compression system was modelled using EES software under various operating situations and the entire system was examined in terms of energy, exergy, economics, and the environment.

CHAPTER 2

BACKGROUND

2.1 MULTI-STAGE VAPOUR COMPRESSION REFRIGERATION SYSTEM

The evaporator and condenser pressure becomes more for lower boiling refrigerants due to which the pressure ratio between evaporator and condenser becomes greater than 4 or 5 which is not acceptable because the volumetric efficiency tends to zero and also the work required for the compression increases. To avoid this problem compression can be done in stages. This can be achieved by employing a flash chamber between the compression stages which can also act as a liquid sub-cooler.

A schematic diagram of the multi-stage vapour compression refrigeration system with flash inter-cooling and a p-h chart of the system is shown in Figures 2.1 and 2.2, respectively. In figure 2.1, the refrigerant at the exit of the evaporator is in a saturated vapour state at 1. The saturated vapour refrigerant then passed through the LPC where saturated vapour gets converted into superheated vapour with an increase in temperature and pressure from evaporator pressure to flash chamber pressure. The de-superheating process takes place after the first stage of compression by the evaporation of a part of liquid refrigerant from the flash chamber at 6.

At state 5 the refrigerant is in a saturated liquid state and then some of its parts are first expanded to the flash chamber pressure through the first expansion valve and the

remaining part is then passed through the flash chamber where the sub-cooling process takes place by the evaporation of the liquid refrigerant in the flash chamber and then it passed through the second expansion valve to the evaporator pressure at 8. The entry of the refrigerant in HPC is at 3 due to de-superheating which results in lower compressor work. Similarly, during the sub-cooling process, the entry at the evaporator is at 8 resulting in an increase in refrigerating effect and consequently, an increase in performance.

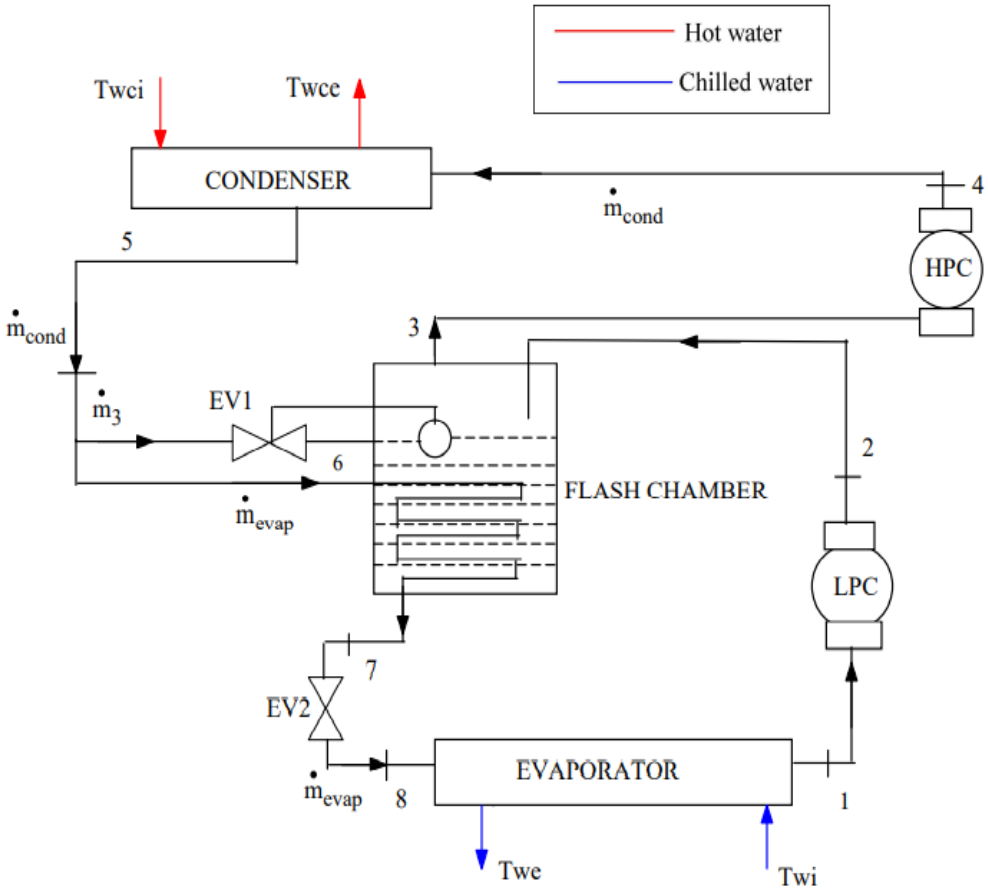

Figure 2.1. Schematic diagram of multi-stage vapour compression refrigeration system

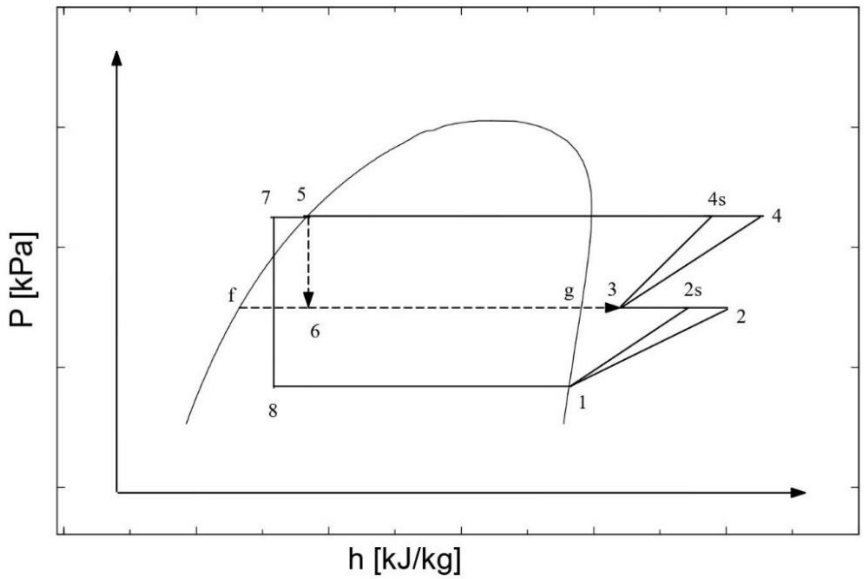

Figure 2.2. P-h diagram of the multi-stage compression system

2.2 THERMODYNAMIC PROPERTIES OF THE REFRIGERANT USED

The properties of refrigerants that are very important to tell whether the refrigerant is a good substitute for the refrigerant presently used in the refrigeration and air-conditioning industry are minimum normal B.P, evaporator & condenser temperature, GWP, ODP, critical temperature and pressure and others. The N.B.P of the refrigerant should be minimum with a freezing point temperature below that of evaporator temperature. From an environmental point of view, the value of ODP and GWP should be minimum. Table 2.1 consists of the thermodynamic properties of refrigerants and at certain operating conditions R134a and R152a show similar properties so, R152a can become an alternate option for R134a due to its low GWP value.

CFC refrigerants is having more value of ODP and GWP and act as greenhouse gases. The best alternative for the CFC refrigerants came with the introduction of HC and HFC refrigerants because of the very less value of ODP and GWP.

Table 2.2 consists of the environmental and physical properties of the refrigerants used in this study where ammonia and R1234ze(E) is having zero value of GWP and ODP but the main concern raised with ammonia is its safety class, because of its slightly flammable behaviour it comes under the safety class of B2. The advantage of using R600a and R290 is that they have very less value of GWP and zero ODP values but they come under the category of A3 because of their flammable nature.

Table 2.1. Refrigerant thermodynamic properties (Baakeem et al. 2018)

Refrigerant	**Molecular Weight**	t_s **(N.B.P) °C**	t_c **(Critical-Temperature) °C**	P_c **(Critical-Pressure) bar**	t_f **(Freezing point) °C**
R717	17.031	-33.35	133.0	112.97	-77.7
R32	52.024	-51.75	78.41	58.3	-136.0
R134a	102.03	-26.15	101.06	40.56	-96.6
R600a	58.13	-11.73	135.0	36.45	-159.6
R290	44.1	-42.1	96.8	42.56	-187.1
R1234ze(E)	114	-18.95	109.4	36.32	-156.0
R152a	66.05	-24.15	113.3	45.2	-117.0
R41	34	-78.2	44.5	58.97	-142.0

Table 2.2. Physical and environmental properties (Baakeem et al. 2018)

Refrigerant	**Type**	**GWP**	**ODP**	**Safety class**	**Flammability**
R717	Natural	0	0	B2	Slightly-flammable
R32	HFC	675	0	A2	Low-flammability
R134a	HFC	1430	0	A1	Non-flammable
R600a	HC	3	0	A3	Flammable
R290	HC	3	0	A3	Flammable
R1234ze(E)	HFO	0	0	A2	Non-flammable
R152a	HFC	140	0	A2	Slightly-flammable
R41	HFC	92	0	B3	Flammable

CHAPTER 3

THERMODYNAMIC ANALYSIS

To create a thermodynamic model, the first and second laws of thermodynamics are extremely important. The mass, energy, and exergy equations are obtained for a multi-stage vapour compression refrigeration system.

While solving the equations, the following assumptions are considered:

1. The pressure drop inside the system components is considered constant with no losses.
2. Changes in kinetic and potential energies are neglected.
3. Constant enthalpy throughout the expansion process.
4. The refrigerant is in saturated condition at the evaporator and condenser outlets.

The following equations are used to model the system after taking the above assumptions:

Material balance $$\sum \dot{m}_{in} - \dot{m}_{out} = 0 \quad (1)$$

Energy balance $$\sum Q - \sum \mathrm{W} - \sum \dot{\mathrm{m}}\mathrm{h} = 0 \quad (2)$$

Exergy balance $$\sum_{in} X - \sum_{out} X - \sum_{heat} X - \sum_{work} X - X_{destroyed} = 0 \quad (3)$$

The EES software facilitates the calculation of refrigerant thermodynamic parameters such as enthalpy, entropy, thermal conductivity, saturation temperature, etc. It is

comprised of both pure and blended substances, making EES suitable for energy/exergy analysis and optimization of any refrigerant in its database. As a result, the system is modelled to study the effect of thermodynamic laws.

3.1 ENERGY ANALYSIS

Table 3.1. Energy equations used in system modelling

Component/Parameter	Energy balance	
Evaporator	$\dot{m}_{evap} = \frac{\dot{Q}_{evap}}{(h_{out} - h_{in})_{evap}}$	(4)
Compressor	$W_{el,LPC} = \frac{W_{LPC}}{\eta_{LPC}}$	(5)
	$W_{el,HPC} = \frac{W_{HPC}}{\eta_{HPC}}$	(6)
	$\eta_{comp} = 0.85 - 0.046667 PR_{comp}$	(7)
Condenser	$\dot{Q}_{cond} = \dot{m}_{cond}(h_{out} - h_{in})$	(8)
Expansion Valve	$h_{in,ev} - h_{out,ev}$	(9)
Flash Chamber	$P_{OPT,int} = \sqrt{\frac{P_{evap} P_{cond} T_{cond}}{T_{evap}}}$	(10)
	$\dot{m}_{cond} = \dot{m}_{evap} + \dot{m}_{fc}$	(11)
	$\dot{m}_{cond} h_5 + \dot{m}_{evap} h_2 = \dot{m}_{cond} h_3 + \dot{m}_{evap} h_7$	(12)

Torrella et al. [4] defined three parameters for an inter-stage configuration:

Sub-cooling parameter	$a = \frac{h_5 - h_7}{h_5 - h_f}$	(13)
De-superheating parameter	$de = \frac{h_2 - h_3}{h_2 - h_g}$	(14)
Mass ratio parameter	$r = \frac{\dot{m}_{cond}}{\dot{m}_{evap}} = \frac{(h_2 - h_5) + a(h_5 - h_f)}{(h_2 - h_5) - b(h_2 - h_g)}$	(15)

Finally, the performance of the system is measured using the equation:

$$COP = \frac{\dot{Q}_{Evap}}{W_{el,LPC} + W_{el,HPC}} \quad (16)$$

3.2 EXERGY ANALYSIS

Exergy destruction for evaporator is calculated using Eq. 17.

$$X_{des,evap} = \sum_{in} X - \sum_{out} X + \dot{Q}_{evap}\left(1 - \frac{T_o}{T_{evap}}\right) \quad (17)$$

Exergy destruction in the evaporator is:

$$X_{des,evap} = \dot{m}_{evap}[(h_8 - h_1) - T_o(s_8 - s_1)] + \dot{Q}_{evap}\left(1 - \frac{T_o}{T_{evap}}\right) \quad (18)$$

Where T_o and T_{evap} are the dead state and evaporation temperature, respectively.

The rate of exergy destruction inside the condenser is given in Eq. 19.

$$X_{des,cond} = \dot{m}_{cond}[(h_4 - h_5) - T_o(s_4 - s_5)] - \dot{Q}_{cond}\left(1 - \frac{T_o}{T_{cond}}\right) \quad (19)$$

The exergy destruction rate of refrigerant in a low-pressure compressor (LPC) is:

$$X_{des,LPC} = \dot{m}_{evap}[(h_1 - h_2) - T_o(s_1 - s_2)] + W_{el,LPC} \quad (20)$$

The exergy destruction rate of refrigerant in a high-pressure compressor (HPC) is:

$$X_{des,HPC} = \dot{m}_{cond}[(h_3 - h_4) - T_o(s_3 - s_4)] + W_{el,HPC} \quad (21)$$

The total exergy destruction rate of the compressor equals:

$$X_{des,comp} = X_{des,LPC} + X_{des,HPC} \quad (22)$$

Exergy destruction of expansion valves are:

$$X_{des,\exp(1)} = \dot{m}_{fc} T_o (s_6 - s_5) \quad (23)$$

$$X_{des,\exp(2)} = \dot{m}_{fc} T_o (s_8 - s_7) \quad (24)$$

Total exergy destruction in expansion valves is:

$$X_{des,exp} = X_{des,\exp(1)} + X_{des,\exp(2)} \quad (25)$$

Exergy destruction in the flash chamber is given by:

$$X_{des,fc} = \dot{m}_{evap}[(h_2 + h_5 - h_7 - h_6) - T_o(s_2 + s_5 - s_7 - s_6)] + \dot{m}_{cond}[(h_6 - h_3) - T_o(s_6 - s_3)] \quad (26)$$

Total exergy destruction for a multi-stage vapour compression refrigeration system will be the total sum of exergy destruction of all the components:

$$X_{des} = X_{des,evap} + X_{des,cond} + X_{des,comp} + X_{des,exp} + X_{des,fc} \quad (27)$$

Exergy efficiency can be calculated using the equation:

$$\eta_{II} = \frac{\dot{Q}_{evap}\left(\frac{T_o}{T_{evap}} - 1\right)}{W_{el}} \quad (28)$$

where, W_{el} is the actual total power consumption by both the compressors.

3.3 ECONOMIC ANALYSIS

For economic analysis, total plant cost is calculated by summing up all the costs involved during modelling i.e., capital costs for each component, maintenance costs, environmental costs and operation costs associated with the system. Table 3.2 represents the equations used to calculate the capital cost of each component separately. To calculate the capital cost of the component, a heat transfer equation is used in which the overall heat transfer coefficient value is assumed for both evaporator and condenser.

The heat transfer equation of the component can be written as:

$$\dot{Q}_{com} = UA\Delta T_m$$

where, ΔT_m is the logarithmic mean temperature difference and A is the area of the component.

Table 3.2. Cost function equations De Paula et al. (2020)

Component	Cost function	
Evaporator	$C_{cap,evap} = \left(516.62 \cdot A_{evap}\right) + 268.45$	(26)
Condenser	$C_{cap,cond} = (516.62 \cdot A_{cond}) + 268.45$	(27)
Expansion valve	$C_{cap,EV} = 114.5 \cdot \dot{m}_{ref}$	(28)
Compressor	$C_{cap,comp} = \left(\frac{573\dot{m}_{ref}}{0.8996 - \eta_{is,comp}}\right) r_p \ (\ln r_p)$	(29)

The total capital cost for the system is:

$$C_{cap,Total} = C_{cap,evap} + C_{cap,cond} + C_{cap,EV} + C_{cap,comp} \quad (30)$$

where $C_{cap,evap}$, $C_{cap,cond}$, $C_{cap,EV}$, and $C_{cap,comp}$ are the capital cost function for the evaporator, condenser, expansion valve, and compressor respectively.

The capital and maintenance cost rate for a multi-stage compression system is calculated in Eq. 31.

$$\dot{C}cm = C_{cap,Total} \cdot \varphi \cdot CRF \quad (31)$$

where φ is the capital and maintenance cost rate and CRF is the capital recovery factor and can be calculated by Eq. 32.

$$CRF = \frac{iR(1+iR)^n}{(1+iR)^{n-1}} \quad (32)$$

where iR is the interest rate and n is the plant lifetime in years.

The operational cost rate for the system is calculated using Eq. 33.

$$\dot{C}oper = \dot{W}_{el} \cdot 365 \cdot T_{oper} \cdot C_{el} \quad (33)$$

where C_{el} is the electricity cost and T_{oper} is the operation time of the system in hours/day. The environmental cost rate for the system is given in Eq. 34.

$$\dot{C}env = \beta \cdot E_{annual} \cdot C_{CO_2} \quad (34)$$

where β is the CO_2 emission factor, C_{CO_2} is the unit damage cost of carbon dioxide emission, and E_{annual} is the electricity consumption by the equipment annually and is calculated by Eq. 35.

$$E_{annual} = 365 \cdot T_{oper} \cdot \left(\frac{\dot{Q}_{evap}}{COP}\right) \quad (35)$$

Table 3.3. Parameters taken for cost calculation

Parameter	Value	Unit	Reference
iR	14	%	[5]
n	15	years	[5]
φ	1.06	(-)	[5]
β	0.968	$kgCO_2/kWh$	[5]
C_{CO_2}	0.09	$USD/kgCO_2$	[5]
C_{elec}	0.075	USD/kWh	[5]

To calculate the overall heat transfer coefficient, a two-phase flow condition is assumed in the design of condenser and evaporator in which many flow regimes are there, whereas in single-phase flow there are only laminar, transition and turbulent flow regimes. The behaviour of the gases-liquid mixtures is strongly dependent on these types of flow regimes. There are certain factors on which the flow regimes and their ranges depend, some of them are:

- Fluid Properties
- Phase change occurrence
- Orientation of the system
- System size

A horizontal pipe is considered while the study of the different flow regimes in which some major flow regimes generally occur are: Stratified smooth, Stratified wavy, Slug flow, and Annular/Dispersed flow regime.

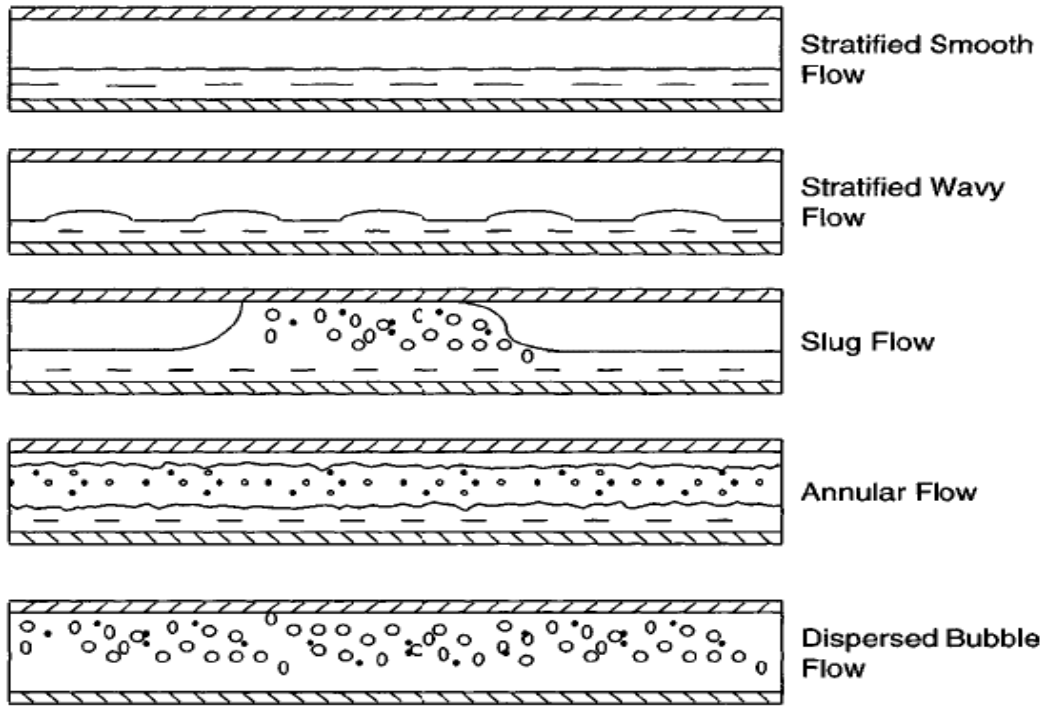

Figure 3.1. Flow regimes inside the horizontal pipe

When the gas flow rate is low the liquid stays at the lower part and gas stays at the upper part of the channel in case of stratified smooth flow. As the gas flow rate increases the state of flow changes.

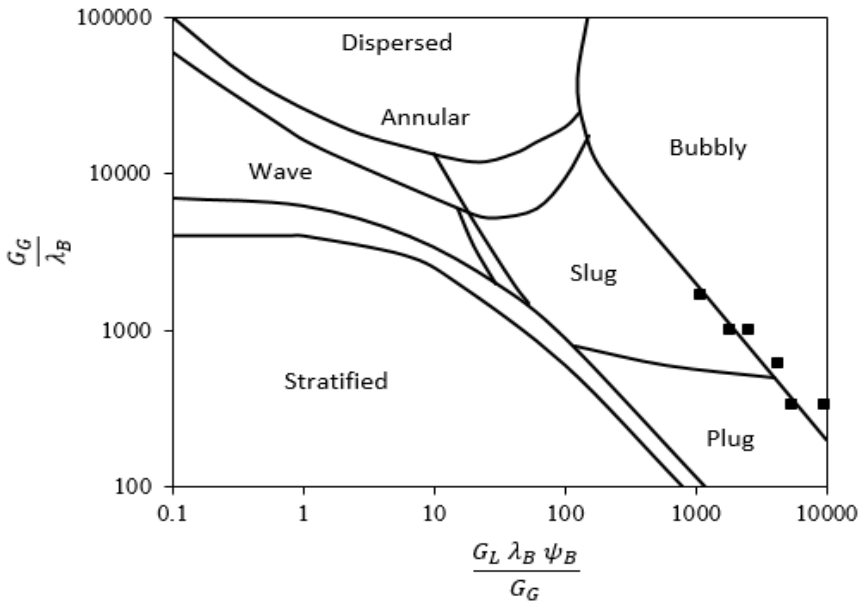

Figure 3.2. Flow regime map of baker (1954)

3.3.1 MODELLING OF TWO-PHASE FLOW

1. Flow Regime Based Models
    - Annular flow model
    - Slug flow model
    - Stratified flow model
    - Dispersed bubbly flow model
2. Flow Regime Independent Models
    - Homogenous Equilibrium Mixture (HEM) model
    - Separated flow model (SFM)
    - Drift flux model (DFM)

In the HEM model, there is only a homogenous mixture present in which all the gases and liquid phases are in thermal equilibrium with equal phase velocities. Whereas, in the case of the stratified flow model the phase velocities are different with a separate motion of the two phases.

During modelling for condenser and evaporator of multi-stage VCRS, a separated flow model is considered for horizontal tubes.

The total pressure gradient inside the tube is calculated using eq.36

$$\left(\frac{dp}{dz}\right) = -\left(\frac{dp}{dz}\right)_F - \left(\frac{dp}{dz}\right)_a - \left(\frac{dp}{dz}\right)_z \tag{36}$$

Where $\left(\frac{dp}{dz}\right)_F$, $\left(\frac{dp}{dz}\right)_a$ and $\left(\frac{dp}{dz}\right)_z$ are the frictional, acceleration and gravity pressure gradients respectively.

The frictional pressure gradient is calculated using eq. 37

$$-\left(\frac{dp}{dz}\right)_F = \frac{2f_{fo}G^2v_f\emptyset_{fo}{}^2}{D} \tag{37}$$

The acceleration pressure gradient is calculated using eq. 38

$$-\left(\frac{dp}{dz}\right)_a = G^2 \frac{dx}{dz} v^* \tag{38}$$

Where v^* can be written as:

$$v^* = \left(\frac{2xv_g}{\alpha} - \frac{2(1-x)v_f}{(1-\alpha)}\right) + \left(\frac{\delta\alpha}{\delta x}\right)_p \left(\frac{(1-x)^2 v_f}{(1-\alpha)^2} - \frac{x^2 v_g}{\alpha^2}\right) \tag{39}$$

The acceleration pressure gradient is calculated using eq. 39

$$-\left(\frac{dp}{dz}\right)_z = \left(\rho_g \alpha + \rho_f (1-\alpha)\right)(g \sin\theta) \tag{40}$$

Two-Phase Frictional Multipliers for homogenous model

$$-\left(\frac{dp}{dz}\right)_F = -\left(\frac{dp}{dz}\right)_{F,fo} \emptyset_{fo}^2 = \frac{2f_{fo}G^2 v_f {\emptyset_{fo}}^2}{D} \tag{41}$$

$$-\left(\frac{dp}{dz}\right)_F = -\left(\frac{dp}{dz}\right)_{F,f} \emptyset_f^2 = \frac{2f_f G^2 (1-x)^2 v_f {\emptyset_f}^2}{D} \tag{42}$$

$$-\left(\frac{dp}{dz}\right)_F = -\left(\frac{dp}{dz}\right)_{F,go} \emptyset_{go}^2 = \frac{2f_{go}G^2 v_g {\emptyset_{go}}^2}{D} \tag{43}$$

$$-\left(\frac{dp}{dz}\right)_F = -\left(\frac{dp}{dz}\right)_{F,g} \emptyset_g^2 = \frac{2f_g G^2 x^2 v_g {\emptyset_g}^2}{D} \tag{44}$$

To calculate two-phase multiplies for the separated flow model Lockhart-Martinelli correlations are used:

$$X^2 = \left(\frac{dp}{dz}\right)_{F,f} \Big/ \left(\frac{dp}{dz}\right)_{F,g} = \emptyset_f^2 / \emptyset_g^2$$

Where *X* is the Lockhart-Martinelli parameter.

Table 3.4. Martinelli Parameter for Different Flow Regimes

Liquid	**Gas**	**Martinelli Parameter**
Turbulent	Turbulent	X_{tt}
Viscous	Turbulent	X_{vt}
Turbulent	Viscous	X_{tv}
Viscous	Viscous	X_{vv}

For turbulent-turbulent flow regimes Martinelli parameter can be written as:

$$X_{tt} = \left(\frac{v_f}{v_g}\right)^{0.5} \left(\frac{\mu_f}{\mu_g}\right)^{0.125} \left(\frac{1-x}{x}\right)^{0.875} \tag{45}$$

For viscous-viscous flow regime:

$$X_{vv} = \left(\frac{v_f}{v_g}\right)^{0.5} \left(\frac{\mu_f}{\mu_g}\right)^{0.5} \left(\frac{1-x}{x}\right)^{0.5} \tag{46}$$

To correlate the frictional multipliers there are relations given by Chisholm and Liard

$$\emptyset_f^2 = 1 + \frac{C}{X} + \frac{1}{X^2} \tag{47}$$

$$\emptyset_g^2 = 1 + CX + X^2 \tag{48}$$

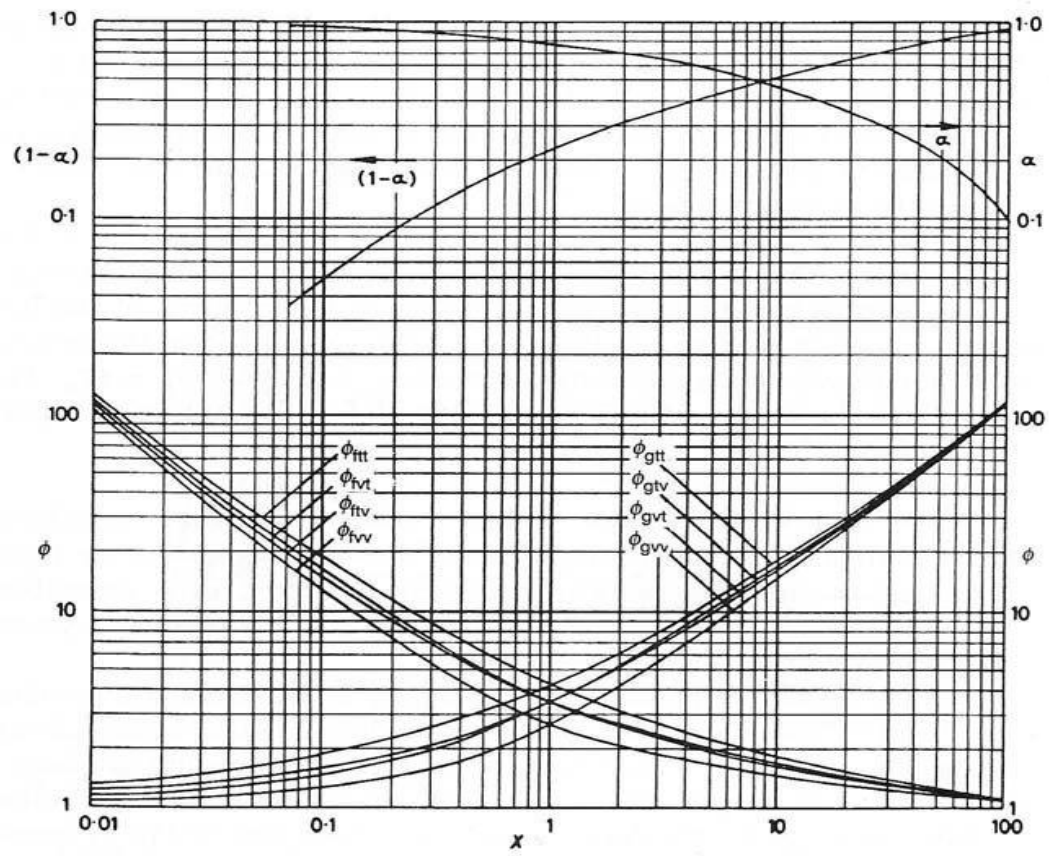

Figure 3.3. Lockhart-Martinelli Correlations Graph

3.3.2 COAXIAL EVAPORATOR

The evaporator is acting as a heat exchanger, where the refrigerant which is flowing inside the tube exchange the heat with the water which is flowing on the outer side of the tube. The heat transfer through the evaporator can be written as:

$$\dot{Q}_{evap} = \dot{m}_{ref}(h1 - h8) = \dot{m}_{w,evap} C_{p,w}(T_{w,i} - T_{w,o}) \quad (49)$$

Where h1 and h8 are the enthalpies at the exit and inlet of the evaporator respectively. $T_{w,i}\ and\ T_{w,o}$ are the temperature of the water inlet and outlet in the shell side of the heat exchanger respectively.

The cooling capacity of the system can be written as:

$$\dot{Q}_{evap} = U_{evap} A_{evap} \Delta T_{m,evap} \quad (50)$$

Where $\Delta T_{m,evap}$ is the logarithmic mean temperature difference, A_{evap} is the area of the equipment and U_{evap} is the overall heat transfer coefficient which can be written as:

$$\frac{1}{U_{evap}} = \frac{1}{h_{tp}} + \frac{D}{h_o D_o} + \frac{ln\left(\frac{D_o}{D}\right)}{2k_{cu}} \quad (51)$$

Where k_{cu} is the thermal conductivity of the copper coils which are used in the evaporator.

The table shows the correlations which are used to calculate the convective heat transfer coefficient for two-phase flow inside the evaporator.

$$h_{tp=} h_{nb} + h_{cv} \quad (52)$$

$$h_{cv} = \frac{0.023 Re_{tp}^{0.8} Pr^{0.4} k_f}{D} \quad (53)$$

$$h_{nb} = \left(\frac{\dot{Q}_e D_b}{k_f T_{avg}}\right)^{0.745} \frac{k_f}{D_b} \left(\frac{\rho_{1,g}}{\rho_{1,f}}\right)^{0.581} Pr^{0.553} 1.25 * 0.207 \quad (54)$$

$$D_b = 0.51 L_a \quad (55)$$

$$h_o = \frac{0.8 Re_w^{0.4} Pr_w^{0.36} k_w}{D_o} \quad (56)$$

Where, h_{cv} and h_{nb} are the forced convection and nucleate boiling heat transfer coefficient.

3.3.3 COAXIAL CONDENSER

The coaxial condenser is also acting as a heat exchanger, where the refrigerant which is flowing inside the tube will exchange the heat with the water which is flowing on the outer side of the tube.
The heat transfer through the condenser can be written as:

$$\dot{Q}_{cond} = \dot{m}_{ref}(h4 - h5) = \dot{m}_{w,cond} C_{p,w} (T_{w,i} - T_{w,o}) \quad (57)$$

Where h5 and h4 are the enthalpies at the exit and inlet of the condenser respectively. $T_{w,i}$ and $T_{w,o}$ are the temperature of the water inlet and outlet in the shell side of the heat exchanger respectively.

The cooling capacity of the system can be written as:

$$\dot{Q}_{evap} = U_{cond} A_{cond} \Delta T_{m,cond} \quad (58)$$

Where $\Delta T_{m,cond}$ is the logarithmic mean temperature difference, A_{cond} is the area of the equipment and U_{evap} is the overall heat transfer coefficient which can be written as:

$$\frac{1}{U_{cond}} = \frac{1}{h_c \pi D_{REF} L_c} + \frac{ln\left(\frac{D_{i,c}}{D_{REF}}\right)}{2\pi k_{cu} L_c} + \frac{\pi D_{o,c} L_c}{h_i} \quad (59)$$

The tube side and shell side convective heat transfer coefficient can be calculated with the help of the following equations:

$$h_1 = h_{lo}\left[1 + \frac{3.8}{Z_c^{0.95}}\right]\left[\frac{\mu_{f,c}}{14\mu_{g,c}}\right]^{(0.0058 + 0.557 P_{rc})} \quad (60)$$

Z_c is the Bond number

$$h_{lo} = 0.023 Re_{lo}^{0.8} Pr_c^{0.4} \frac{k_c}{D} \quad (61)$$

$$h_{iii} = \frac{1.32}{Re_{lo}^{(1/3)}}\left[\frac{\rho_{f,c}\ 9.81\ (\rho_{f,c} - \rho_{g,c})\ k_c^3}{\mu_{f,c}^2}\right]^{(1/3)} \quad (62)$$

$$h_c = h_1 + h_{iii}$$

$$h_i = 0.023\left[\frac{G_{c,w}\ D_o}{\mu_{f,c}}\right]^{0.8}\left[\frac{cp_w \mu_{f,c}}{k_{c,w}}\right]^{0.4} \quad (63)$$

3.4 ENVIRONMENTAL ANALYSIS

From an environmental point of view, the amount of carbon emission is very important either it can be a direct or indirect source of emission. The total equivalent warming impact factor (TEWI) can be a factor which helps to tell how much carbon is emitted and it can be calculated by Eq. 64.

$$TEWI = TEWI_{DIRECT} + TEWI_{INDIRECT} \quad (64)$$

$TEWI_{DIRECT}$ and $TEWI_{INDIRECT}$ is calculated using Eq. 37. and Eq. 38. respectively.

$$TEWI_{direct} = E_{annual} \cdot \beta \cdot L_{time} \quad (65)$$

where L_{time} is the life span of the plant.

$$TEWI_{indirect} = \left(GWP \cdot \dot{m}_{ref} \cdot L_{rate} \cdot L_{time}\right) + \left(GWP \cdot \dot{m}_{ref} \cdot (1 - \alpha_{rec})\right) \quad (66)$$

where $\dot{m}_{ref}$ is the total refrigerant mass running in the complete refrigeration system, L_{rate} is the rate of refrigerant emitted annually, and α_{rec} is the refrigerant life recovery rate. Table 3.5 represents the data taken for environmental analysis.

Table 3.5. Values taken for calculation of TEWI parameter

Parameter	Value	Reference
L_{rate}	0.0125	[5]
α_{rec}	0.7	[5]
β (kgCo2)	0.082	[5]
T_{oper} (hours)	8	[5]

CHAPTER 4

4.1 MODEL VALIDATION

The present model is validated with the model developed by [20] in which they theoretically investigate the multi-stage compression system and optimized the model with the help of EES software. They considered eight refrigerants in their study to optimize the model taking four parameters into account. Those four parameters were T_e, T_C, a, and de. The direct search method is used for the optimization of the model to get maximum COP at evaporation and condensation temperature of 10°C and 40°C respectively. Table 3 presents the results obtained in the present study and reference study. There is a 0.47% difference in maximum COP of ammonia whereas R1234ze(E) refrigerant system shows a maximum difference in COP of 1.13%.

Table 4.1. Model validation of multi-stage compression system

Refrigerant	**Baakeem et al. (2018)**		**Present work**		**Difference (%)**	
	COP_{max}	η_{II} (%)	COP_{max}	η_{II} (%)	COP_{max}	η_{II}
R717	6.17	32.7	6.199	32.86	+0.47	+0.489
R134a	6.01	31.9	6.048	32.06	+0.63	+0.501
R1234ze(E)	6.01	32.2	6.078	32.21	+1.13	+0.031

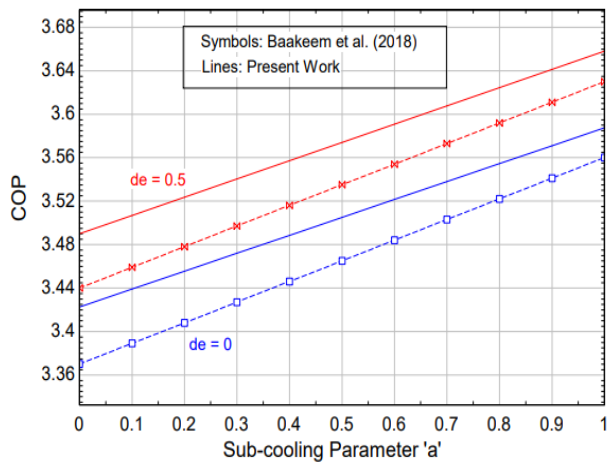

Figure 4.1. Model validation for Ammonia multi-stage compression system

4.2 INPUT PARAMETERS

The thermodynamic analysis of a multi-stage compression system is carried out in the present work using EES software. Baakeem et al. [20] assumed the following input parameters listed in the table before performing operations.

Table 4.2. Input parameters for system modelling

Parameters	Value
Evaporation Temperature, $\boldsymbol{T_{evap}}$ (℃)	0
Condensation Temperature, $\boldsymbol{T_{cond}}$ (℃)	45.0
Sub-cooler Efficiency, (%)	80
LPC Efficiency, (%)	91
Cooling Load, $(\boldsymbol{kW})$	1

Table 4.3. Input parameters for economic and environmental analysis

Parameters	Values
Inner Diameter of Evaporator Tube	0.0158 (m)
Outer Diameter of Evaporator Tube	0.0191 (m)
Inner Diameter of Condenser Tube	0.00952 (m)
Outer Diameter of Condenser Tube	0.0208 (m)
Evaporator Inlet and Outlet Water Temperature	30 and 15 $(°C)$
Condenser Inlet and Outlet Water Temperature	20 and 30 $(°C)$

CHAPTER 5

RESULTS AND DISCUSSION

5.1 MODEL OPTIMIZATION

To converge the findings, EES software employs several optimization approaches. When there is only one degree of freedom, the golden search method is employed to discover the minimum or maximum. Because there is more than one variable in this study, the conjugate direction approach is employed to maximise the system's performance (COP). In EES, the conjugate direction approach is also known as the direct search method, because it searches for an optimum value of, X_1 while keeping, X_2, X_3, X_4, and so on constant. To maximise the performance of the multi-stage system, four independent variables are taken into account: T_e, T_c, a, and de. The system is optimised by keeping the evaporator's lower and upper temperatures at -20 and 10°C, respectively. The temperature limit for the condenser is fixed between 40 and 60°C. During the optimization, the "a" and "de" parameters vary between 0 and 1.

Table 5.1. Optimization results for different refrigerants

Refrigerant	**Optimum Conditions**				COP_{max}	η_{ii} (%)	X_{des} (W)	C_{total} (USD)	TEWI (kgCo2)
	T_{evap} (°C)	T_{cond} (°C)	**a**	**de**					
R717	10	40	1	1	6.199	32.86	53.9	676.1	579.3
R134a	10	40	1	1	6.048	32.02	57.93	840.6	859.4
R32	10	40	1	1	5.871	31.12	62.5	798.3	736.7
R1234ze(E)	10	40	1	0	6.078	32.17	57.2	902	591.7
R41	10	40	1	1	4.602	24.4	107.5	830.1	792.2
R152a	10	40	1	1	6.155	32.63	54.99	824.1	609.4
R600a	10	40	1	1	6.123	32.58	55.23	797.2	584.9
R290	10	40	1	1	5.993	31.73	59.36	891.7	600.5

5.2 THE INFLUENCE OF “a” AND “de” PARAMETERS ON THE COP

Figure 5.1-(a) shows that for refrigerants R717, as the “de” parameter increases with an increase in parameter “a” the performance increases for the R717 refrigerant system. At constant sub-cooler efficiency of 80% as the “de” parameter increases from 0-0.5 and 0.5-1, the increase in performance is 1.99% and 2.26%, respectively. After optimization, the COP increases by 70.959% for the R717 refrigerant system.

For the R32 refrigerant system, figure 5.1-(b) shows that the system's performance is increasing with an increase in “a” and “de” parameters. As the “de” parameter changes from 0-0.5 and 0.5-1, there is a 1.03% and 1.223% increase in the performance of the system, respectively. It can be seen from figure 5.1-(c) that for refrigerant R152a, there is a slight increment of 0.109% and 0.1365% in the performance of the system as the “de” parameter changes from 0-0.5 and 0.5-1 respectively, at constant sub-cooler efficiency.

The multi-stage system shows opposite behaviour in the case of R134a, R41, and R290 refrigerants. As the de-superheating parameter increases from 0-1, the system's performance tends to decrease with 0.056% decrement for the R134a refrigerant system, 1.836-2.577% decrement in the case of the R41 refrigerant system, and 0.845% of decrement in the case of R290 refrigerant system.

When a multi-stage compression system is operating with R1234ze and R600a refrigerants, the performance of the multi-stage system is independent of the change in the de-superheating parameter and increases with an increase in the sub-cooling parameter. At constant sub-cooler efficiency, the performance of the multi-stage system is 3.609 and 3.565 for R1234ze and R600a, respectively. In the case of the R152a refrigerant system, the change in performance is very significant with an increase in the de-superheating parameter. Fig shows that only 0.109% and 0.1365% increment in COP when the de-superheating parameter changes between 0-0.5 and 0.5-1, respectively.

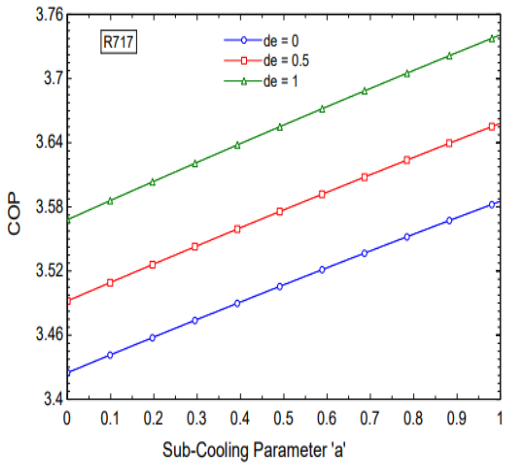
R717
de = 0
de = 0.5
de = 1
COP
Sub-Cooling Parameter 'a'

(a)

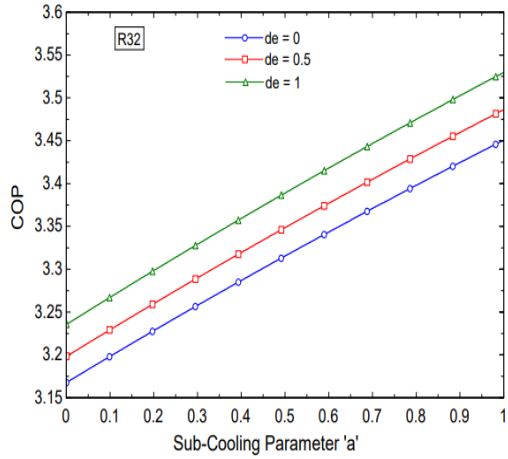
R32
de = 0
de = 0.5
de = 1
COP
Sub-Cooling Parameter 'a'

(b)

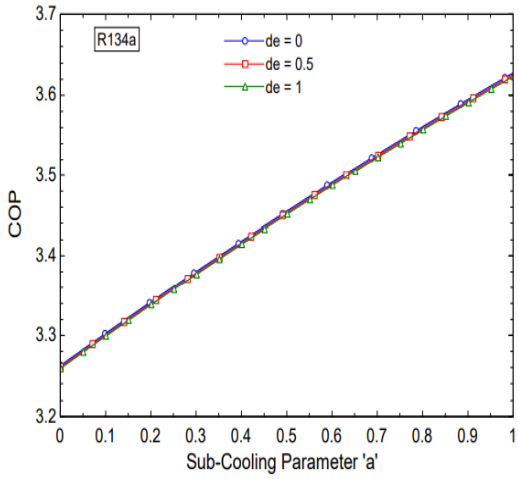
R134a
de = 0
de = 0.5
de = 1
COP
Sub-Cooling Parameter 'a'

(c)

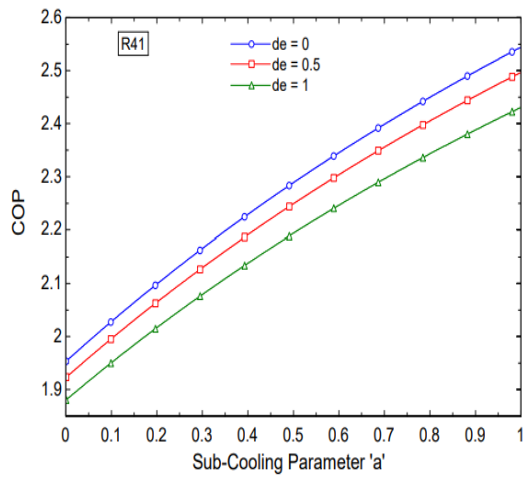
R41
de = 0
de = 0.5
de = 1
COP
Sub-Cooling Parameter 'a'

(d)

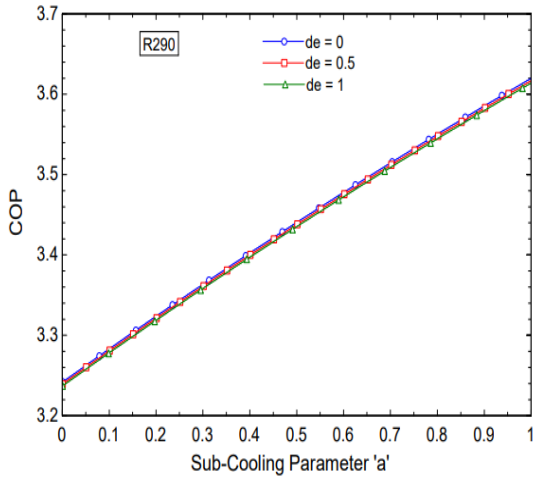
R290
de = 0
de = 0.5
de = 1
COP
Sub-Cooling Parameter 'a'

(e)

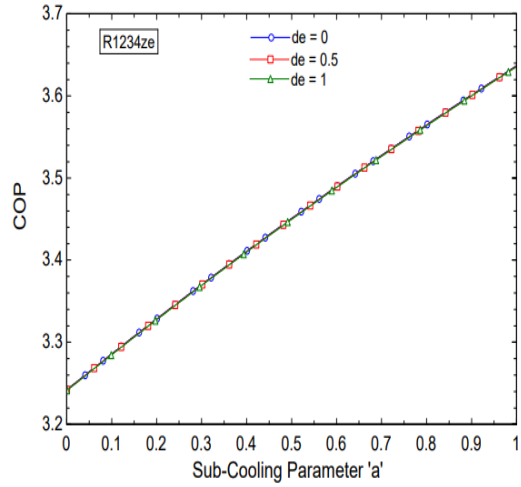
R1234ze
de = 0
de = 0.5
de = 1
COP
Sub-Cooling Parameter 'a'

(f)

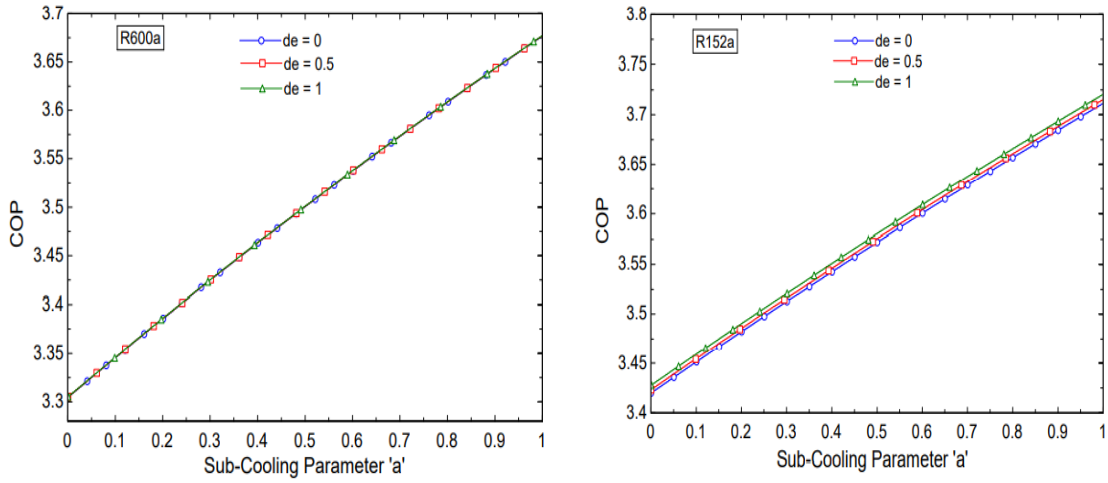

(g) (h)

Figure 5.1. The influence of "a" and "de" parameters on the system's performance

5.3 THE INFLUENCE OF "a" AND "de" PARAMETERS ON THE EXERGETIC EFFICIENCY

In a multi-stage compression, the exergy efficiency depends upon certain factors. Some of them are evaporation temperature, dead state temperature, sub-cooling parameter, and de-superheating parameters. This study focuses on how the system efficiency is affected when there is variation in "a" and "de" parameters. From figure 5.2-(a), with an increase in the "a" parameter, the exergetic efficiency is increasing. For R717, R32, and R152a refrigerant systems, the exergetic efficiency increment is 2.027-2.22%, 1.028-1.024%, and 0.0895-0.149% respectively when the de-superheating varies between 0-0.5 and 0.5-1 respectively.

For refrigerants R41, R134a, and R290, an adverse effect can be seen when compared to R717, R32, and R152a. The exergetic efficiency decreases with an increase in the "de" parameter as the "a" parameter increases. For R134a and R290 refrigerant systems, the decrease in exergetic efficiency is negligible. When the "de" parameter varies between 0-1, only 0.03-0.06% and 0.092% decrement in efficiency can be seen, respectively. For the R41 refrigerant system, 1.827-2.587% of decrement in exergy efficiency is seen when the "de" parameter varies between 0 to 1. In the case of R1234ze and R600a, the effect of the "de" parameter on exergetic efficiency is nearly zero. The second law efficiency increases when the sub-cooling parameter increases from 0 to 1.

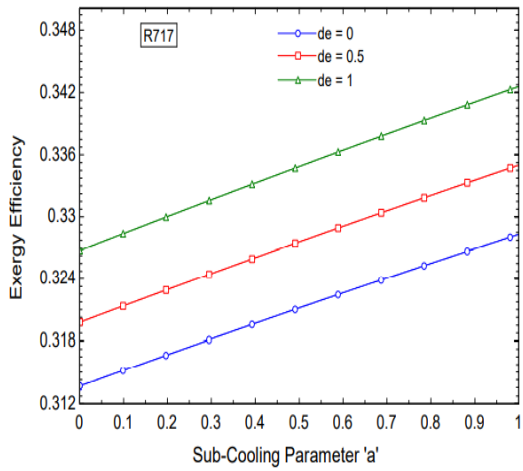
R717
de = 0
de = 0.5
de = 1
Exergy Efficiency
Sub-Cooling Parameter 'a'

(a)

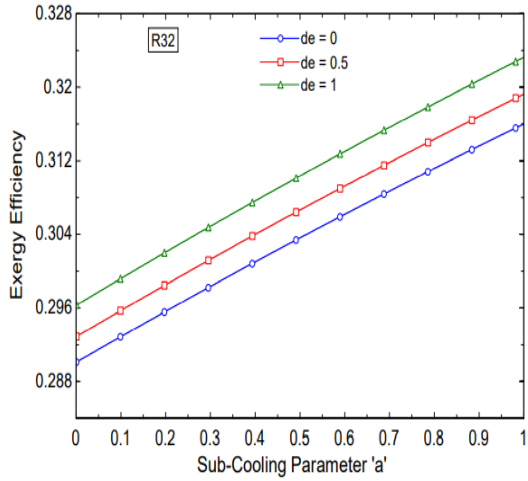
R32
de = 0
de = 0.5
de = 1
Exergy Efficiency
Sub-Cooling Parameter 'a'

(b)

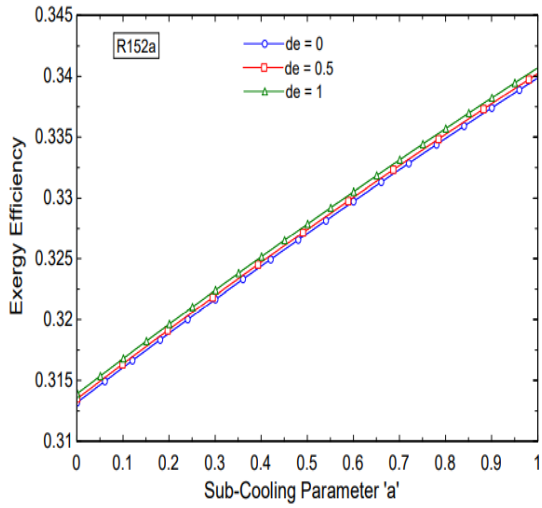
R152a
de = 0
de = 0.5
de = 1
Exergy Efficiency
Sub-Cooling Parameter 'a'

(c)

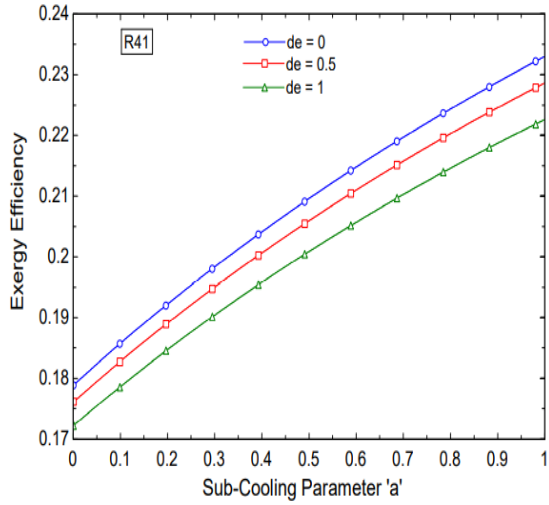
R41
de = 0
de = 0.5
de = 1
Exergy Efficiency
Sub-Cooling Parameter 'a'

(d)

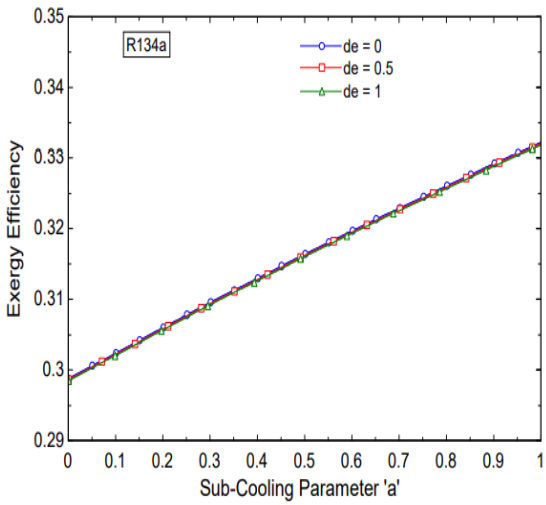
R134a
de = 0
de = 0.5
de = 1
Exergy Efficiency
Sub-Cooling Parameter 'a'

(e)

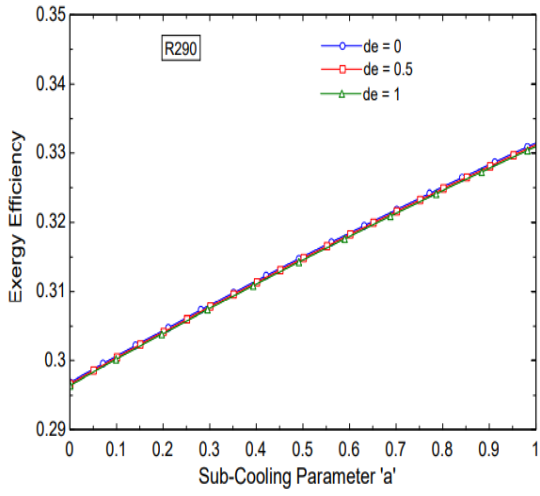
R290
de = 0
de = 0.5
de = 1
Exergy Efficiency
Sub-Cooling Parameter 'a'

(f)

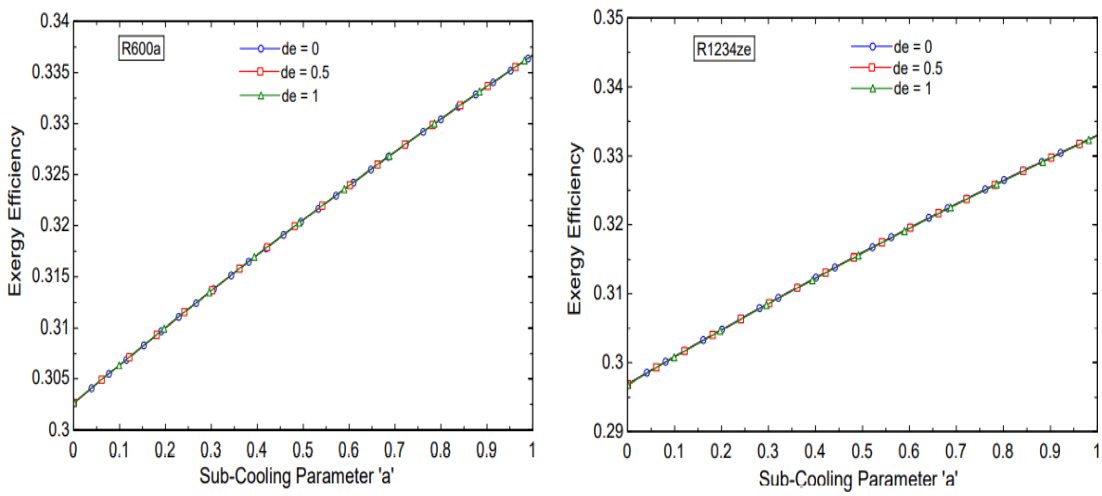

(g) (h)

Figure 5.2. The influence of “a” and “de” parameters on the system’s efficiency

5.4 THE INFLUENCE OF “a” AND “de” PARAMETERS ON THE EXERGY DESTRUCTION RATE

When a system's exergy destruction rate rises, it results in increased power consumption. As a result, it is very critical to examine the system in terms of exergy destruction rate. For refrigerants R717, R32, and R152a, the exergy destruction rate decreases with an increase in sub-cooling and de-superheating parameters. Results show an exergy destruction rate decrement of 4.719-5.40% for R717, 2.25-2.71 for R32, and 0.286-0.382% for R152a when the de-superheating parameter varies between 0 to 1.

Figure 5.3 shows that for R600a and R1234ze refrigerant systems, there is a negligible amount of change in exergy destruction rate when the de-superheating parameter increases.

For R134a, R290, and R41 refrigerant systems as the system's performance decreases with an increase in the de-superheating parameter, the exergy destruction rate increases by 2.25-2.71%, 0.1776-0.1779%, and 3.0879-4.2675%, respectively.

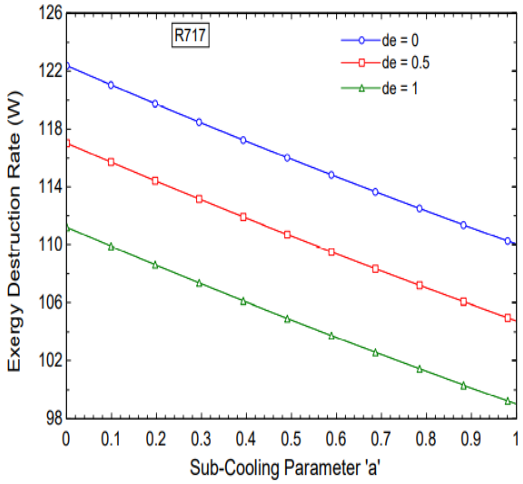
R717
de = 0
de = 0.5
de = 1
Exergy Destruction Rate (W)
Sub-Cooling Parameter 'a'

(a)

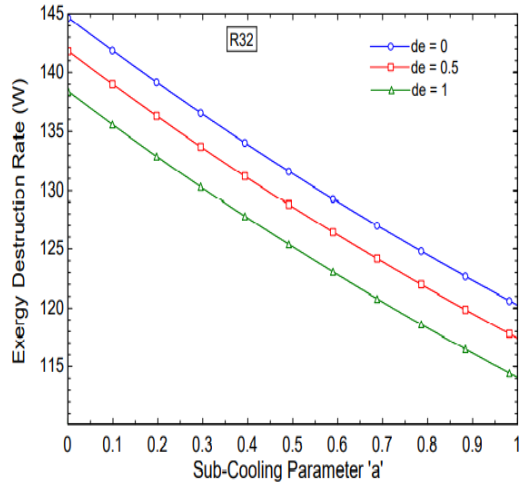
R32
de = 0
de = 0.5
de = 1
Exergy Destruction Rate (W)
Sub-Cooling Parameter 'a'

(b)

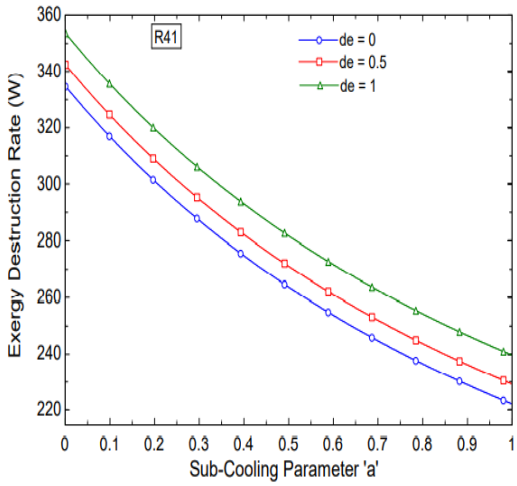
R41
de = 0
de = 0.5
de = 1
Exergy Destruction Rate (W)
Sub-Cooling Parameter 'a'

(c)

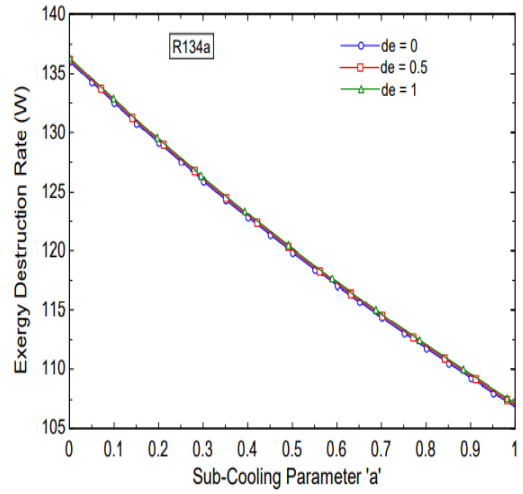
R134a
de = 0
de = 0.5
de = 1
Exergy Destruction Rate (W)
Sub-Cooling Parameter 'a'

(d)

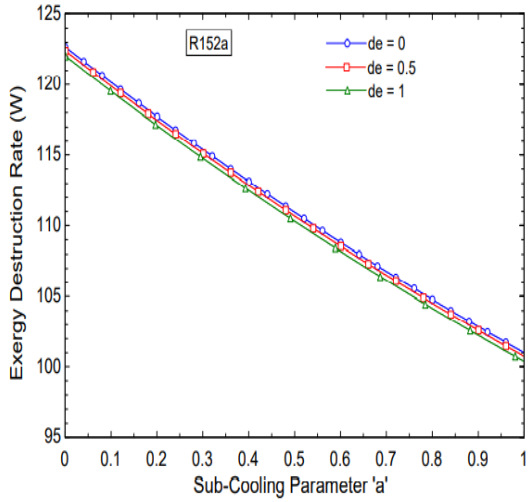
R152a
de = 0
de = 0.5
de = 1
Exergy Destruction Rate (W)
Sub-Cooling Parameter 'a'

(e)

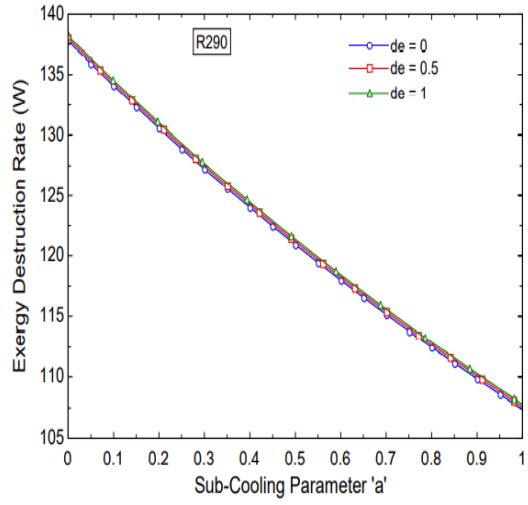
R290
de = 0
de = 0.5
de = 1
Exergy Destruction Rate (W)
Sub-Cooling Parameter 'a'

(f)

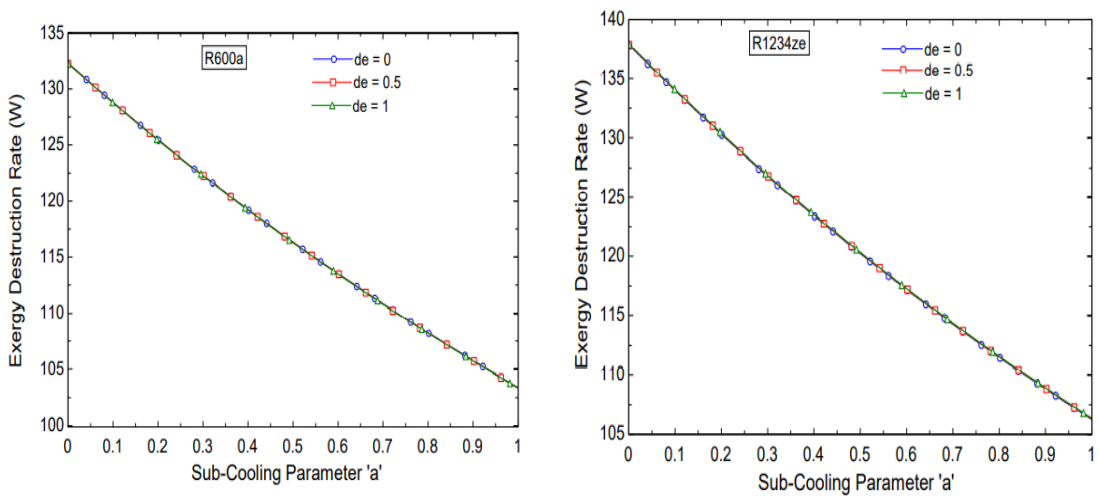

(g) (h)

Figure 5.3. The influence of “a” and “de” parameters on the destruction rate of exergy

5.5 THE INFLUENCE OF “a” AND “de” PARAMETERS ON THE TOTAL CAPITAL COST

For refrigerants R717, R32, and R152a, the total capital cost decreases with an increase in sub-cooling and de-superheating parameters. Results show a total capital cost increment of 0.0796% for R717, 0.513% for R32, and 0.06555% for R152a when the de-superheating parameter varies between 0 to 1. Figure 5.4 shows that for R600a and R1234ze refrigerant systems, there is a negligible amount of change in the total capital cost when the de-superheating parameter increases.

For R134a, R290, and R41 refrigerant systems as the system's performance decreases with an increase in the de-superheating parameter, the total capital cost increase by 0.025%, 0.06%, and 1.81%, respectively with an increase in “de” parameter from 0 to 1. After optimization, there is an increase in total capital cost of an average of 7% for R717, R134a, and R32 refrigerants.

For refrigerant R1234ze, R290, and R152a there is an average increase of 10% in the total capital cost after optimization and there can be seen a very less increase in the cost of 4% in the case of R41.

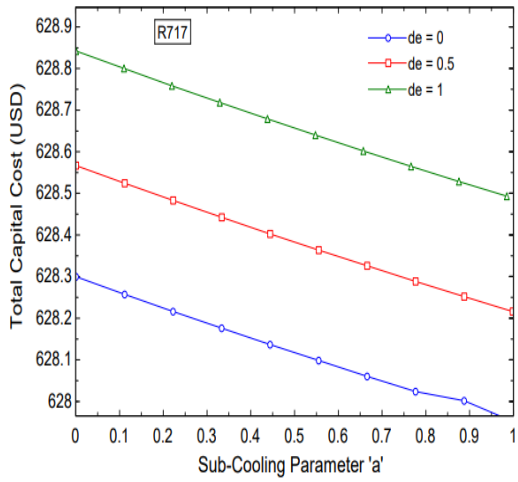
R717
de = 0
de = 0.5
de = 1
Total Capital Cost (USD)
Sub-Cooling Parameter 'a'

(a)

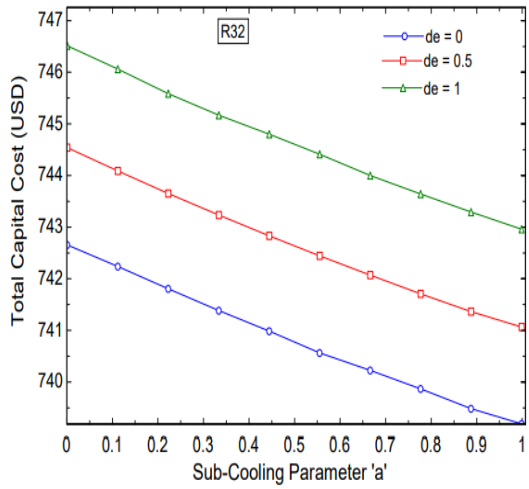
R32
de = 0
de = 0.5
de = 1
Total Capital Cost (USD)
Sub-Cooling Parameter 'a'

(b)

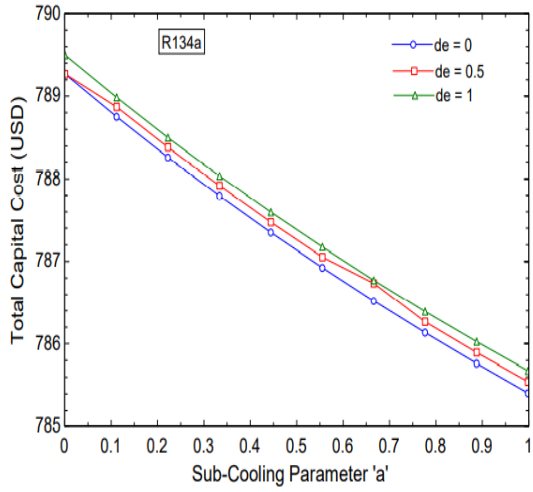
R134a
de = 0
de = 0.5
de = 1
Total Capital Cost (USD)
Sub-Cooling Parameter 'a'

(c)

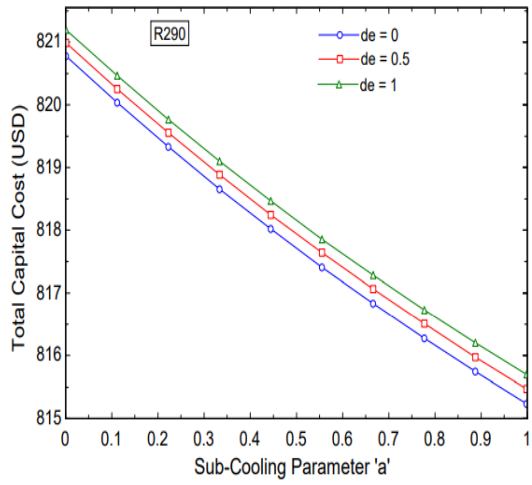
R290
de = 0
de = 0.5
de = 1
Total Capital Cost (USD)
Sub-Cooling Parameter 'a'

(d)

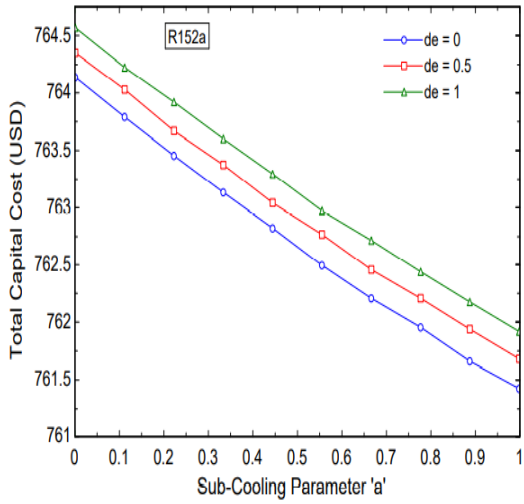
R152a
de = 0
de = 0.5
de = 1
Total Capital Cost (USD)
Sub-Cooling Parameter 'a'

(e)

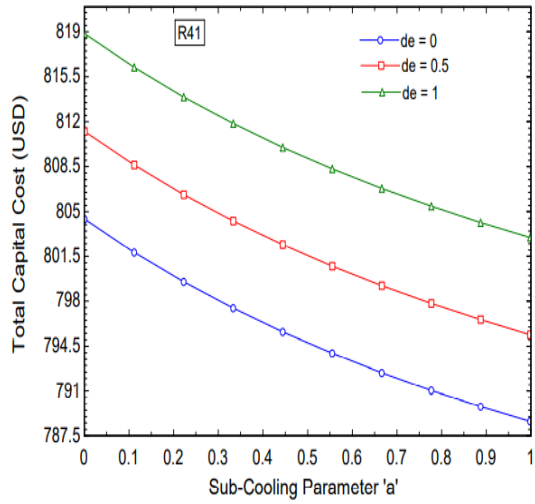
R41
de = 0
de = 0.5
de = 1
Total Capital Cost (USD)
Sub-Cooling Parameter 'a'

(f)

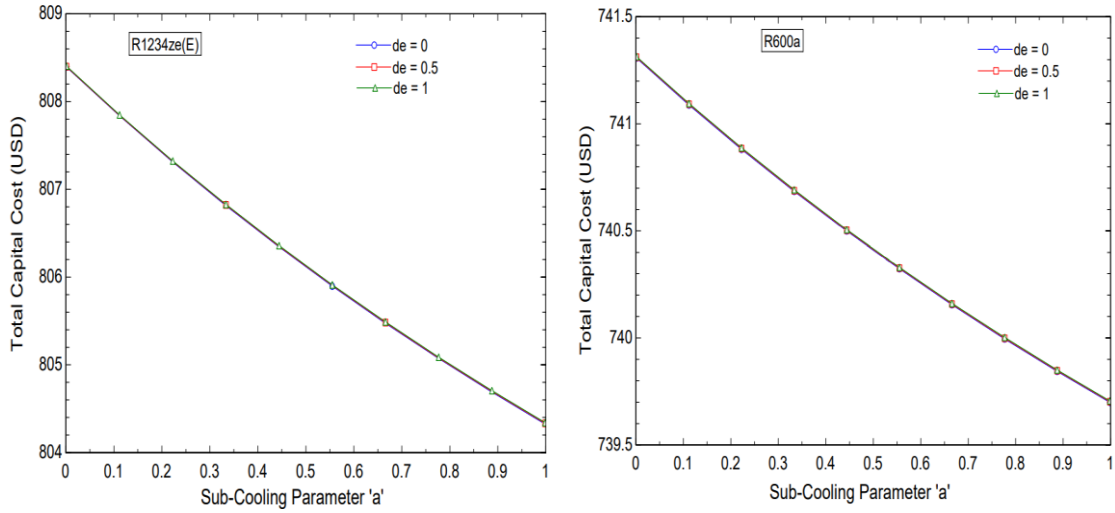

(g) (h)

Figure 5.4. The influence of "a" and "de" on the total capital cost

5.6 THE INFLUENCE OF "a" AND "de" PARAMETERS ON THE TOTAL EQUIVALENT WARMING IMPACT FACTOR (TEWI)

For refrigerants R717, R32, and R152a, the total capital cost decreases with an increase in sub-cooling and de-superheating parameters. Results show a TEWI decrement of 4% for R717, 5% for R32, and 0.2% for R152a when the de-superheating parameter varies between 0 to 1. Figure 5.5 shows that for R600a and R1234ze refrigerant systems, there is a negligible amount of change in the total capital cost when the de-superheating parameter increases.

For R134a, R290, and R41 refrigerant systems as the system's performance decreases with an increase in the de-superheating parameter, the total capital cost increase by 0.025%, 0.06%, and 1.81%, respectively with an increase in "de" parameter from 0 to 1. After optimization, there is a decrease in the TEWI factor of an average of 35% for R717, R134a, and R32 refrigerants. For refrigerant R1234ze, R290, and R152a there is an average increase of 40% in the TEWI factor after optimization and there can be seen an increase in the TEWI factor of 43% in the case of R41.

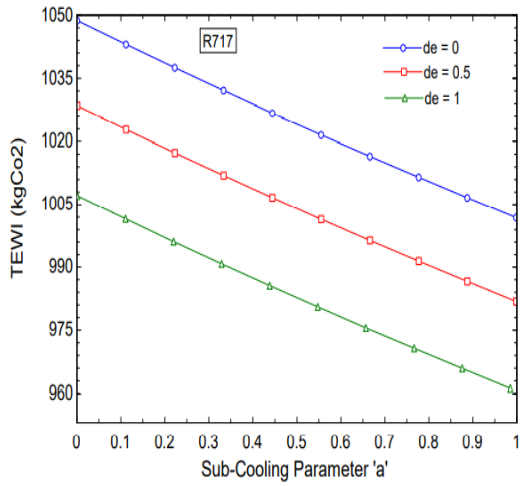
R717
de = 0
de = 0.5
de = 1
TEWI (kgCo2)
Sub-Cooling Parameter 'a'

(a)

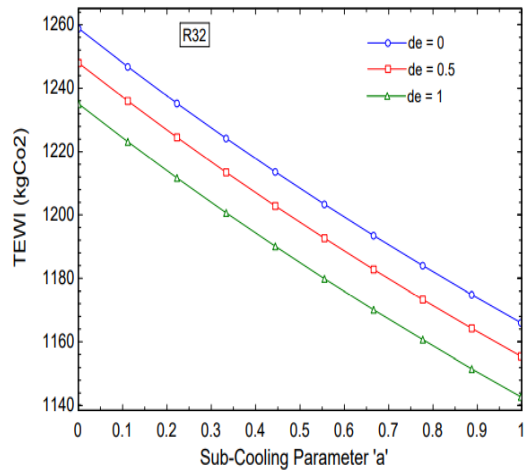
R32
de = 0
de = 0.5
de = 1
TEWI (kgCo2)
Sub-Cooling Parameter 'a'

(b)

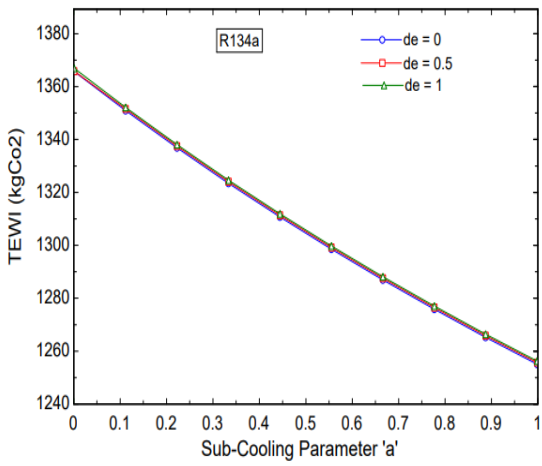
R134a
de = 0
de = 0.5
de = 1
TEWI (kgCo2)
Sub-Cooling Parameter 'a'

(c)

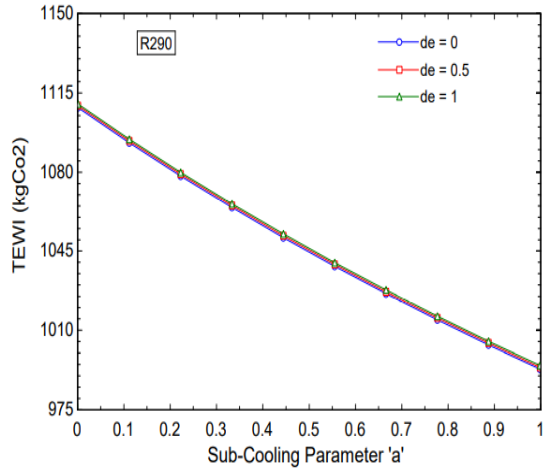
R290
de = 0
de = 0.5
de = 1
TEWI (kgCo2)
Sub-Cooling Parameter 'a'

(d)

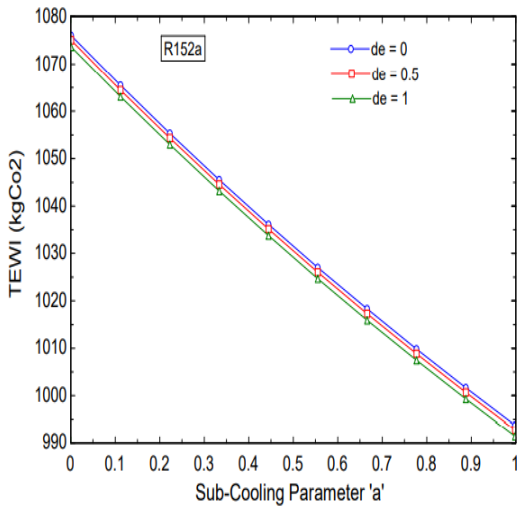
R152a
de = 0
de = 0.5
de = 1
TEWI (kgCo2)
Sub-Cooling Parameter 'a'

(e)

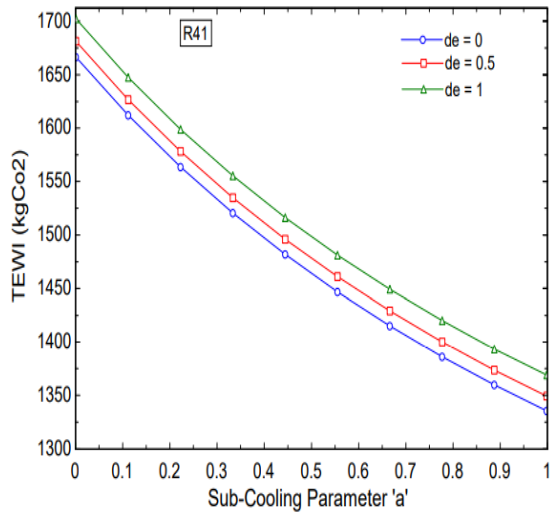
R41
de = 0
de = 0.5
de = 1
TEWI (kgCo2)
Sub-Cooling Parameter 'a'

(f)

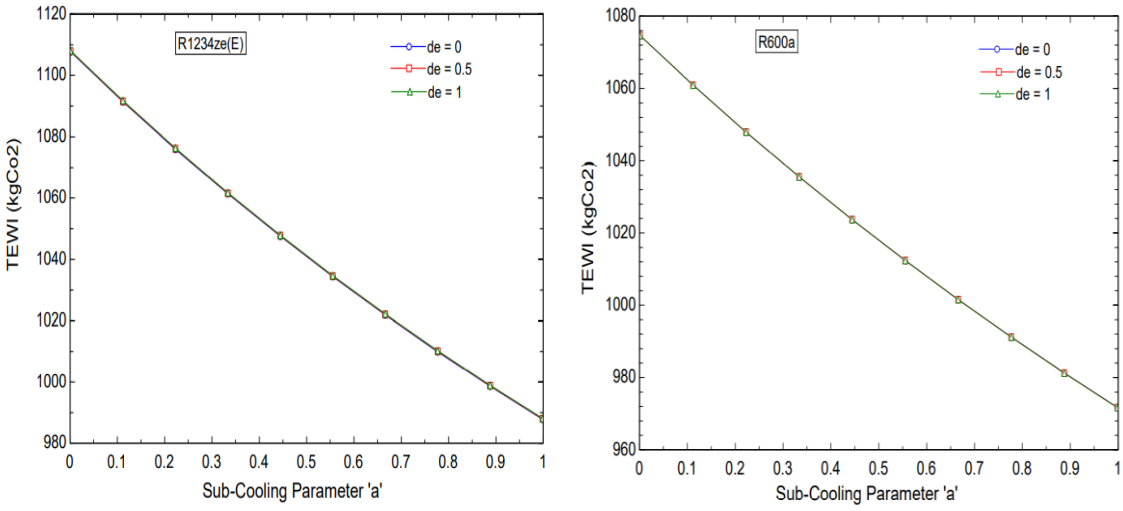

(g) (h)

Figure 5.5. The influence of “a” and “de” parameters on the total equivalent warming impact factor

CHAPTER 6

CONCLUSIONS

The R717, R32, R290, R1234ze(E), R152a, R41, R134a, and R600a refrigerants are considered in the theoretical study of the multi-stage VCRS utilising EES software to investigate the exergy rate of the system. The system's performance is optimised based on the four parameters, namely, T_{evap}, T_{cond}, a, and de, and, as a result, the minimum exergy destruction rate and second-law efficiency are assessed.

The following conclusions are drawn from the findings:

- R717 among all other refrigerants used performs better in terms of COP, second law efficiency, and exergy destruction rate. Results show that the second law efficiency and the exergy destruction rate of R717 are 33.21% and 107 W respectively. After optimization of system performance, the efficiency of the system increases by 1.05% with a reduction of 49.61% in the exergy destruction rate.

- The system's second law efficiency improves as the de-superheating parameter is increased for R717, R32, and R152a refrigerant systems and also the exergy destruction rate reduces with an increase in the de-superheating parameter.

- When the "de" parameter is increased, R134a, R290, and R41 have an unfavourable influence on the second law efficiency and exergy destruction rate. The effect of increasing the “de” parameter on R1234ze and R600a refrigerants is negligible.

- After optimization of the system performance, the maximum COP came out for R717 refrigerant with an increment of 70.96%. Also, with an increase in parameters “a” and “de”, system efficiency increases by 2.027-2.22%.

- At sub-cooler efficiency, evaporation temperature, and condensation temperature, R41 refrigerant shows less reduction in exergy destruction rate as compared to the other seven refrigerants.

- After optimization of the system, the capital cost of the system increases and the TEWI factor decreased with an average value of 38% for all the refrigerants.

- With an increased “de” parameter the capital cost of the system decreases with an average value of 0.08% for R717, R32 and R152a. R1234ze(E) and R600a show a negligible change in the capital cost with an increase in the “de” parameter at constant sub-cooler efficiency.

R717 outperforms the other seven refrigerants with maximum performance with lesser exergy destruction, according to the findings. R1234ze(E) can be used as a substitute for R717 because there is almost the same percentage decrease in the TEWI factor for both i.e., 41% and the total capital cost increment of R1234ze(E) after optimization is 12.05% which is nearly the capital cost increment of R717 and R41 refrigerant is not recommended for usage since its exergy destruction rate is higher with more increase in the percentage of total capital cost.

6.1 SCOPE AND FUTURE WORK

- To improve the performance of the system new azeotropic mixtures can be used as one of them is R454B.
- A liquid sub-cooler can be implemented separately to cool down the temperature and compressor work.
- Modelling of evaporator and condenser can also be done on ANSYS software to carry out heat transfer related results.

APPENDIX

EES CODE FOR MULTI-STAGE VAPOUR COMPRESSION REFRIGERATION SYSTEM

```
FUNCTION f_foc(Re_foc)

    f_foc = (64/Re_foc)
    IF(Re_foc<1187) THEN RETURN

    f_foc = (0.3164/Re_foc)
    IF (Re_foc>1187) THEN RETURN
END

Te=0
Tc=43
Pe=P_sat(R41,T=Te)
Pc=P_sat(R41,T=Tc)
P=(((Pe*Pc*(Tc+273))/(Te+273))^0.5)

h1=Enthalpy(R41,P=Pe,x=1)
s1=Entropy(R41,P=Pe,x=1)
s1=s2s
s2s=Entropy(R41,T=T2s,P=P)
h2s=Enthalpy(R41,T=T2s,P=P)

nc1=(h2s-h1)/(h2-h1)
nc1=0.91
h2=Enthalpy(R41,P=P,T=T2)

de=(h2-h3)/(h2-hg)
hg=Enthalpy(R41,P=P,x=1)
de=0.9985

h3=Enthalpy(R41,T=T3,P=P)
s3=Entropy(R41,T=T3,P=P)
s3=s4s
s4s=Entropy(R41,T=T4s,P=Pc)
h4s=Enthalpy(R41,T=T4s,P=Pc)
```

```
nc2=(h4s-h3)/(h4-h3)
nc2=(0.85-(0.046667*(Pc/P)))

h5=Enthalpy(R41,P=Pc,x=0)

a=(h5-h7)/(h5-hf)
hf=Enthalpy(R41,P=P,x=0)
a=0.8

h5=h6
h7=hf7
h7=h8
h7=Enthalpy(R41,T=T7,P=Pc)
{hf7=Enthalpy(R41,T=T7,x=0)}

Qe_dot=1
Qe_dot=me_dot*(h1-h8)
(mc_dot*h5)+(me_dot*h2)=(mc_dot*h3)+(me_dot*h7)
mc_dot = me_dot+m3

Wc1_dot=me_dot*(h2-h1)
Wc2_dot=mc_dot*(h4-h3)
W_dot=Wc1_dot+Wc2_dot
Wel1_dot=Wc1_dot/nc1
Wel2_dot=Wc2_dot/nc2
Wel_dot=Wel1_dot+Wel2_dot

COP = Qe_dot/Wel_dot

n_ii=((Qe_dot*(((To+273)/(Te+273))-1))/Wel_dot)

To=25

"Exergy Analysis"

"Evaporator"

Xe = me_dot*((h8-h1)-((To+273)*(s8-s1)))+Qe_dot*(1-((To+273)/(Te+273)))
h8=hf8+(x8*(h1-hf8))
hf8=Enthalpy(R41,T=Te,x=0)
s8=sf8+(x8*(s1-sf8))
sf8=Entropy(R41,T=Te,x=0)
```

"Condenser"

Xc = mc_dot*((h4-h5)-((To+273)*(s4-s5)))-Qc_dot*(1-((To+273)/(Tc+273)))
Qc_dot = mc_dot*(h4-h5)
s5=Entropy(R41,T=Tc,x=0)
h4=Enthalpy(R41,T=T4,P=Pc)
s4=Entropy(R41,T=T4,P=Pc)

"Compressor"

X_c1 = me_dot*((h1-h2)-((To+273)*(s1-s2)))+Wel1_dot
X_c2 = mc_dot*((h3-h4)-((To+273)*(s3-s4)))+Wel2_dot
s2=Entropy(R41,T=T2,P=P)
X_comp = X_c1+X_c2

"Expansion valves"

X_ev1 = m3*(To+273)*(s6-s5)
h6 = hf+(x6*(hg-hf))
s6 = sf+(x6*(sg-sf))
sf=Entropy(R41,P=P,x=0)
sg=Entropy(R41,P=P,x=1)
X_ev2 = me_dot*(To+273)*(s8-s7)
s7=Entropy(R41,T=T7,P=Pc)
X_ev = X_ev1+X_ev2

"Flash Chamber"

X_fc = m + n
m = me_dot*((h2+h5-h7-h6)-((To+273)*(s2+s5-s7-s6)))
n = mc_dot*((h6-h3)-((To+273)*(s6-s3)))
X_des = (Xe + Xc + X_comp + X_ev + X_fc)*1000
r = mc_dot/me_dot

"Compressor"

C_c2=((573*mc_dot)/(0.8996-(nc2)))*(r_p2)*(ln(r_p2)) " Capital cost of HPC in USD"
r_p2=(Pc/P)

"Expansion Valve"

```
C_TEV1=114.5*me_dot
C_TEV2=114.5*mc_dot
C_TEV=((C_TEV1+C_TEV2))

"Condenser"

C_cond = (516.62*A_c)+268.45
Qc_dot = (U_c*A_c*T_mc)
{U_c = 0.5}
Twc_i = 20
Twc_e = 30
Tx = Tc-Twc_i
Ty = Tc-Twc_e
T_mc = (Tx-Ty)/(ln(Tx/Ty))

"Evaporator"

C_evap = (516.62*A_e)+268.45
Qe_dot = (U*A_e*T_me)
{U_e = 0.5}
Twe_i = 30
Twe_e = 15
Tk = Twe_i - Te
Td = Twe_e - Te
T_me = (Tk-Td)/(ln(Tk/Td))
C_total = C_evap + C_cond + C_TEV + C_c2

"Pressure drop"

mu1f=Viscosity(R41,T=Te,x=0)
mu1=Viscosity(R41,T=Te,x=1)
v1f=Volume(R41,T=Te,x=0)
v1=Volume(R41,T=Te,x=1)
deltaP = ((deltaP_f + deltaP_a + deltaP_z))                "kPa"
deltaP_f = ((2*(f_fo)*(G^2)*(v1f)*L*(Int))/(D*(x2-x1)))
Int=integral(((phi_fo)^2),x,x1,x2,0.01)
x1 = 0.05
x2 = 0.98

{((phi_fo)^2) = ((1-x)^(7/4))*((phi_f)^2)}
{((phi_fo)^2) = ((f_f)*((1-x)^2)*((phi_f)^2))/(f_fo)}
```

```
{((phi_f)^2) = 1+(C/Z)+(C/(Z^2))
C = 20
Z = ((v1f/v1)^0.5)*((mu1f/mu1)^0.125)*(((1-x)/x)^0.875)}

G = ((me_dot)*4)/(pi*(D^2)*L)                                    "Mass Flux"
L = 6                                                            "Length in m"
D = 0.0158                                                       "Inner dia of tube in m"
f_fo = (0.079/((Re_fo)^0.25))          "Friction factor when only fluid is flowing"
{f_f =  (0.079/((Re_f)^0.25))}
Re_fo = (G*D)/(mu1f)                   "Reynolds number for only fluid flowing inside
the tube"
{Re_f = (G*D*(1-x))/(mu1f)}

 t = ((v1f/v1)^0.5)*((mu1f/mu1)^0.125)
((phi_fo)^2) = (((1-x)^1.75)+(20*(x^0.875)*((1-x)^0.875))/t)+((20*(x^1.75))/(t^2))
"Frictional multiplier for fluid flow only"

deltaP_a = (G^2)*v1f*(r_2)
r_2 = 500                  "From nelson-martenelli graph"
deltaP_z = 0
(P_up) = deltaP + Pe                    "Pressure above 0C"

(T_up)=T_sat(R41,P=P_up)          "Saturation temp corresponding to the pressure
which was before drop"
T_avg = (((T_up)+(Te))/2)

"Properties at T_avg"

k_f=Conductivity(R41,T=T_avg,x=0)
Pr=Prandtl(R41,T=T_avg,x=0)
rho_1f=Density(R41,T=T_avg,x=0)
rho_1g=Density(R41,T=T_avg,x=1)
mu_1fNew=Viscosity(R41,T=T_avg,x=0)
mu_1New=Viscosity(R41,T=T_avg,x=1)
sigma=SurfaceTension(R41,T=T_avg)
h1_f=Enthalpy(R41,T=T_avg,x=0)
h1_new=Enthalpy(R41,T=T_avg,x=1)

h_tp = (h_cv + h_nb)" h_tp = two phase, h_cv = forced convection , h_nb = nucleate
boiling"
```

```
h_cv = ((0.023*((Re_tp)^0.8)*(Pr^0.4)*(k_f))/(d_i))/1000
d_i = D                                          "Inner dia of tube"

Z = ((rho_1g/rho_1f)^0.5)*((mu_1fNew/mu_1New)^0.1)*(((1-(x_q))/x_q)^0.9)     "
Martinelli parameter"
x_q= 0.5                                         "Quality"

F = 1+(2/(Z)^0.88)                               " two phase convection multiplier factor"
Re_foNew = (G*D*0.5)/(mu_1fNew)
Re_tp = (F^(1/0.8))*(Re_foNew)

h_nb = ((K^0.745)*S*h_pb)
(K^0.745) = 1/(1+(0.875*eff)+(0.518*(eff^2))-(0.159*(eff^3))+(0.7907*(eff^4)))
""
eff = (h_cv)/(S*(h_pb))
""
S = (1-(1/exp(eps)))/eps
"Supression factor"
eps = ((((rho_1f)*(cp_l)*(T_avg+273))/((rho_1g)*((h1_new)-
h1_f)))^1.25)*((h_cv)/k_f)*(L_a)*(5/10^5)
cp_l=Cp(R41,T=T_avg,x=0)

L_a = ((2*sigma)/(9.81*((rho_1f)-(rho_1g))))^0.5
h_pb =
(((Qe_dot)*(D_b)/((k_f)*(T_avg+273)))^0.745)*((k_f)/D_b)*(((rho_1g)/rho_1f)^0.581)
*(Pr^0.533)*(1.25*207) "divided by 1000 nahi kiya kuki Qe_dot kW mai hai"
D_b = 0.51*(L_a)

"Waterside h.t coefficient"

t_m = ((Twe_i) + (Twe_e))/2                      "Mean temp of water"
h_o=(0.8*((Re_w)^0.4)*((Pr_w)^0.36)*((k_w)/D_o))/1000
D_o = 0.0191
Re_w = ((G_w)*(D_o))/(mu_w)

Pr_w=Prandtl(Water,T=t_m,x=0)
k_w = Conductivity(Water,T=t_m,x=0)
mu_w=Viscosity(Water,T=t_m,x=0)
G_w = ((mw_dot)/A_w)
A_w = (pi*((D_o)^2))/4

Qe_dot = mw_dot*(cp_w)*((Twe_i)-(Twe_e))
```

```
cp_w=Cp(Water,T=t_m,x=0)

"overall h.t coefficient"

(1/U) = (1/h_tp)+((D)/((h_o)*D_o))+(D*(ln((D_o)/D))/(2*k_cu))
{(1/U) = (1/(h_tp*pi*D*L_c))+((ln(D_ie/D))/(2*pi*k_cu*L_c))+(1/h_o*pi*D_o*L_c)}
k_cu = 0.387
{D_ie = 0.0168}

P_reduced = Pe_new/P_critical
Pe_new=P_sat(R41,T=T_avg)
P_critical=P_crit(R41)

"Condenser pressure drop"

hgc=Enthalpy(R41,T=Tc,x=1)
mufc=Viscosity(R41,T=Tc,x=0)
mugc=Viscosity(R41,T=Tc,x=1)
rhogc=Density(R41,T=Tc,x=1)
rhofc=Density(R41,T=Tc,x=0)
vfc=Volume(R41,T=Tc,x=0)
vgc=Volume(R41,T=Tc,x=1)

f_foc = f_foc(Re_foc)

G_c = (mc_dot)/Aci
Aci = ((pi*(D^2))/4)

Re_foc = (G*D)/mufc
Re_goc = (G*D)/mugc

{f_foc = 64/Re_foc}
f_goc = 64/Re_goc

deltaP_Ffoc =  ((f_foc)*((G_c)^2)*(vfc))/(2*D)
deltaP_Fgoc = ((f_goc)*((G_c)^2)*(vgc))/(2*D)

delta_PFc = beta * (deltaP_Fgoc)
beta = ((theta+(2*(1-theta)*x_c))*((1-(x_c))^(1/3)))+((x_c)^3)
theta = ((64/0.314)*(mufc)*(vfc))/((mugc^0.25)*(vgc)*(((G_c)*D)^0.75))

Int2=integral(delta_PFc,x_c,0.5,0.9,0)
```

P_down = Pc - delta_PFc
T_down=T_sat(R41,P=P_down)

Tc_new = (Tc-(T_down/2))
Pc_new=P_sat(R41,T=Tc_new)

"Properties at Tc_new"

Pr_c=Prandtl(R41,T=Tc_new,x=0)
mufc_n=Viscosity(R41,T=Tc_new,x=0)
mugc_n=Viscosity(R41,T=Tc_new,x=1)
rhofc_n=Density(R41,T=Tc_new,x=0)
rhogc_n=Density(R41,T=Tc_new,x=1)
vfc_n=Volume(R41,T=Tc_new,x=0)
vgc_n=Volume(R41,T=Tc_new,x=1)
sigma_cn=SurfaceTension(R41,T=Tc_new)
k_c=Conductivity(R41,T=Tc_new,x=0)
hgc_n=Enthalpy(R41,T=Tc_new,x=1)

"tube side"

h_1 = (h_lo)*(1+(3.8/(Z_c)^0.95))*(((mufc_n)/(14*mugc_n))^(0.0058+0.557*Pr_c))
h_lo = 0.023*((Re_lo)^0.8)*((Pr_c)^0.4)*((k_c)/D)
Z_c = ((1/(1-x_q))^0.8)*((Pred_c)^0.4) "Bond Number"
Pred_c = (Pc_new)/(P_critical)

Re_lo = ((G_c*D*(1-x_q))/mufc_n)

h_iii = ((1.32/((Re_lo)^(1/3)))*((((rhofc_n*9.81*(rhofc_n - rhogc_n)*((k_c)^3))/(mufc_n)^2))^(1/3)))

h_c = (h_1 + h_iii)/1000

"Water side/outside"

((h_i*D_o)/k_cw) = 0.023*(((G_cw*D_o)/(mufc_w))^0.8)*(((cpc_w*mufc_w)/k_cw)^0.4)
cpc_w=Cp(Water,T=T_wc,x=0)
k_cw=Conductivity(Water,T=T_wc,x=0)
T_wc = Twc_i + ((Twc_i - Twc_e)/2) "Properties of water at this temp and other one is temp rise ka mean"

```
G_cw = ((mc_dot)*4)/(pi*((D_o)^2))
mufc_w=Viscosity(Water,T=T_wc,x=0)

{(1/U_c) = (1/h_c)+((D)/((h_i)*D_o))+(D*(ln((D_o)/D))/(2*k_cu))}

D_REF = 0.00794
D_ic = 0.00952
D_oc = 0.0208

(1/U_c) =
(1/(h_c*pi*D_REF*L_c))+((ln(D_ic/D_REF))/(2*pi*k_cu*L_c))+(1/h_i*pi*D_oc*L_c
)
L_c = 6

"Environmental analysis"

TEWI=TEWI_direct+TEWI_indirect
"total equivalent warming impact [kgCO2]"

TEWI_indirect=(E_annual*B*L_time)
L_time=15                                          "life of the refrigeration
system [years]"
E_annual  = 365*T_oper*(Qe_dot/COP)
B = 0.082                        "kgCo2/kWh"

TEWI_direct=(GWP*(m_ref)*L_rate*L_time)+(GWP*(m_ref)*(1-a_recup))
a_recup=0.7
"refrigerant life recovery rate [%]"
L_rate=0.0125
"annual rate of refrigerant emitted [%]"
GWP=140
{m_ref=rho_ref*((3.14/4)*(D_ref)^2)*L
D_ref=6.36/1000  "mm"
L=17 "meters"
rho_ref=660     "kg/m^3"}
m_ref=0.38
"refrigerant charge in kg"

T_oper = 8
```

REFERENCES

[1] A. H. Nasution, H. Ambarita, H. V. Sihombing, E. Y. Setiawan and H. Kawai, "The effect of stage number on the performance of a vapor compression refrigeration cycle using refrigerant R32," in *IOP Conference Series: Materials Science and Engineering*, 2020.

[2] J. Gill and J. Singh, "Energy analysis of vapor compression refrigeration system using mixture of R134a and LPG as refrigerant," *International Journal of Refrigeration*, 2017.

[3] A. H. Mosaffa and L. G. Farshi, "Exergoeconomic and environmental analyses of an air conditioning system using thermal energy storage," *Applied Energy*, vol. 162, pp. 515-526, 2016.

[4] E. Torrella, J. A. Larumbe, R. Cabello, R. Llopis and D. Sanchez, "A general methodology for energy comparison of intermediate configurations in two-stage vapour compression refrigeration systems," *Energy*, vol. 36, no. 7, pp. 4119-4124, 2011.

[5] C. H. de Paula, W. M. Duarte, T. T. M. Rocha, R. N. de Oliveira, R. d. P. Mendes and A. A. Torres Maia, "Thermo-economic and environmental analysis of a small capacity vapor compression refrigeration system using R290, R1234yf, and R600a," *International Journal of Refrigeration*, vol. 118, pp. 250-260, 2020.

[6] B. Morad, M. Gadalla and S. Ahmed, "Energetic and exergetic comparative analysis of advanced vapour compression cycles for cooling applications using alternative refrigerants," *International Journal of Exergy*, vol. 26, no. 1-2, pp. 226-246, 2018.

[7] C. Nikolaidis and D. Probert, "Exergy-method analysis of a two-stage vapour-compression refrigeration-plants performance," *Applied Energy*, vol. 60, no. 4, pp. 241-256, 1998.

[8] I. J. Esfahani, Y. T. Kang and C. Yoo, "A high efficient combined multi-effect evaporation–absorption heat pump and vapor-compression refrigeration part 1: Energy and economic modeling and analysis," *Energy*, vol. 75, pp. 312-326, 2014.

[9] R. Roy and B. K. Mandal, "Thermo-economic analysis and multi-objective optimization of vapour cascade refrigeration system using different refrigerant combinations," *Journal of Thermal Analysis and Calorimetry*, vol. 139, no. 5, pp. 3247-3261, 2019.

[10] A. Arora, B. B. Arora, B. D. Pathak and H. L. Sachdev, "Exergy analysis of a Vapour Compression Refrigeration system with R-22, R-407C and R-410A," *International Journal of Exergy*, vol. 4, no. 4, pp. 441-454, 2007.

[11] A. Arora and S. Kaushik, "Energy and exergy analyses of a two-stage vapour compression refrigeration system," *International Journal of Energy Research*, vol. 34, pp. 907-923, 2010.

[12] A. Bhamidipati, S. Pendyala and R. Prattipati, “Performance evaluation of multi pressure refrigeration system using R32,” *Materials Today: Proceedings,* vol. 28, no. 4, pp. 2405-2410, 2020.

[13] J. U. Ahamed, R. Saidur and H. H. Masjuki, “A review on exergy analysis of vapor compression refrigeration system,” 2011.

[14] E. Mancuhan, “A comprehensive comparison between low and medium temperature application refrigerants at a two-stage refrigeration system with flash intercooling,” 2019.

[15] K. K. Singh, R. Kumar and A. Gupta, “Comparative energy, exergy and economic analysis of a cascade refrigeration system incorporated with flash tank (HTC) and a flash intercooler with indirect subcooler (LTC) using natural refrigerant couples,” *Sustainable Energy Technologies and Assessments,* vol. 39, 2020.

[16] A. S. Dalkilic and S. Wongwises, “A performance comparison of vapour-compression refrigeration system using various alternative refrigerants,” *International Communications in Heat and Mass Transfer,* vol. 37, no. 9, pp. 1340-1349, 2010.

[17] E. Bilgen and H. Takahashi, “Exergy analysis and experimental study of heat pump systems,” *Exergy, An International Journal,* vol. 2, no. 4, pp. 259-265, 2002.

[18] J. Yu, S. Momoki and S. Koyama, “Experimental study of surface effect on flow boiling heat transfer in horizontal smooth tubes,” *International Journal of Heat and Mass Transfer,* vol. 42, pp. 1909-1918, 1996.

[19] M. M. Shah, “Comprehensive correlations for heat transfer during condensation in conventional and mini/micro channels in all orientations,” *International Journal of Refrigeration,* vol. 67, pp. 22-41, 2016.

[20] S. S. Baakeem, J. Orfi and A. Alabdulkarem, “Optimization of a multistage vapor-compression refrigeration system for various refrigerants,” *Applied Thermal Engineering,* vol. 136, pp. 84-96, 2018.

[21] A. Alabdulkarem, R. Eldeeb, Y. Hwang, V. Aute and R. Radermacher, “Testing, simulation and soft-optimization of R410A low-GWP alternatives in heat pump system,” *International Journal of Refrigeration,* vol. 60, pp. 106-117, 2015.